

Localization, Stability, and Resolution of Topological Derivative Based Imaging Functionals in Elasticity*

Habib Ammari[†], Elie Bretin[‡], Josselin Garnier[§], Wenjia Jing[†], Hyeonbae Kang[¶], and Abdul Wahab^{||}

Abstract. The focus of this work is on rigorous mathematical analysis of the topological derivative based detection algorithms for the localization of an elastic inclusion of vanishing characteristic size. A filtered quadratic misfit is considered, and the performance of the topological derivative imaging functional resulting therefrom is analyzed. Our analysis reveals that the imaging functional may not attain its maximum at the location of the inclusion. Moreover, the resolution of the image is below the diffraction limit. Both phenomena are due to the coupling of pressure and shear waves propagating with different wave speeds and polarization directions. A novel imaging functional based on the weighted Helmholtz decomposition of the topological derivative is, therefore, introduced. It is thereby substantiated that the maximum of the imaging functional is attained at the location of the inclusion and the resolution is enhanced and proves to be the diffraction limit. Finally, we investigate the stability of the proposed imaging functionals with respect to measurement and medium noises.

Key words. elasticity imaging, elastic waves, topological derivative, topological sensitivity, localization, resolution

AMS subject classifications. Primary, 35L05, 35R30, 74B05; Secondary, 47A52, 65J20

DOI. 10.1137/120899303

1. Introduction. We consider the inverse problem of identifying from boundary measurements the location of a small elastic inclusion in a homogeneous isotropic background medium. The main motivations of this work are nondestructive testing (NDT) of elastic structures for material impurities [14], exploration geophysics [1], and medical diagnosis, in particular, for detection of potential tumors of diminishing size [26].

The long-standing problem of anomaly detection has been addressed using a variety of techniques including small volume expansion methods [10, 9], MUSIC-type algorithms [5], and time-reversal techniques [4, 7]. The focus of the present study is on the topological derivative based anomaly detection algorithms for elasticity. As shown in [6], in antiplane elasticity, the topological derivative based imaging functional performs well and is robust with respect to

*Received by the editors November 19, 2012; accepted for publication (in revised form) July 22, 2013; published electronically November 5, 2013. This work was supported by the ERC Advanced Grant Project MULTIMOD-267184 and Korean Ministry of Education, Science, and Technology through grant NRF 2010-0017532.

<http://www.siam.org/journals/siims/6-4/89930.html>

[†]Department of Mathematics and Applications, Ecole Normale Supérieure, 75005 Paris, France (habib.ammari@ens.fr, wjing@dma.ens.fr).

[‡]Institut Camille Jordan, INSA de Lyon, Villeurbanne Cedex 69621, France (elie.bretin@insa-lyon.fr).

[§]Laboratoire de Probabilités et Modèles Aléatoires & Laboratoire Jacques-Louis Lions, Université Paris VII, 75205 Paris Cedex 13, France (garnier@math.jussieu.fr).

[¶]Department of Mathematics, Inha University, Incheon 402-751, Korea (hbkang@inha.ac.kr).

^{||}Department of Mathematics, COMSATS Institute of Information Technology, Wah Cantt. 47040, Pakistan (wahab@ciitwah.edu.pk).

noise and sparse or limited view measurements. The objective of this work is to extend this concept to the general case of linear isotropic elasticity. The analysis is much more delicate in the general case than in the scalar case because of the coupling between the shear and pressure waves.

The concept of topological derivative (TD), initially proposed for shape optimization in [16, 25, 13], has been recently applied to the imaging of small anomalies; see, for instance, [14, 15, 18, 19, 20, 21, 24] and references therein. However, its use in the context of imaging has been heuristic and lacks mathematical justifications, notwithstanding its usefulness.

In a prior work [6], acoustic anomaly detection algorithms based on the concept of TD are analyzed, and their performance is compared with that of different detection techniques. Moreover, a stability and resolution analysis is carried out in the presence of measurement and medium noises.

The aim of this work is to analyze the ability of the TD based sensitivity framework for detecting elastic inclusions of vanishing characteristic size. Precisely, our goal is threefold: (i) to perform a rigorous mathematical analysis of the TD based imaging; (2) to design a modified imaging framework based on the analysis. In the case of a density contrast, the modified framework yields a TD based imaging functional, i.e., deriving from the TD of a discrepancy functional. However, in the case where the Lamé coefficients of the small inclusion are different from those of the background medium, the modified functional is rather of a Kirchhoff type. It is based on the correlations between, separately, the shear and compressional parts of the backpropagation of the data and those of the background solution. It cannot be derived as the TD of a discrepancy functional; and (3) to investigate the stability of the proposed imaging functionals with respect to measurement and medium noises.

In order to put this work in a proper context, we emphasize some of its significant achievements. A trial inclusion is created in the background medium at a given search location. Then, a discrepancy functional is considered (cf. section 3), which is the elastic counterpart of the filtered quadratic misfit proposed in [6]. The search points that minimize the discrepancy between measured data and the fitted data are then sought. In order to find its minima, the misfit is expanded using the asymptotic expansions due to the perturbation of the displacement field in the presence of an inclusion versus its characteristic size. The first order term in the expansion is then referred to as the TD of the misfit (cf. section 3.1), which synthesizes its sensitivity relative to the insertion of an inclusion at a given search location. We show that its maximum, which corresponds to the point at which the insertion of the inclusion maximally decreases the misfit, may not be at the location of the true inclusion (cf. section 3.2). Further, it is revealed that its resolution is low due to the coupling of pressure and shear wave modes having different wave speeds and polarization directions. Nevertheless, the coupling terms responsible for this degeneracy can be canceled out using a modified imaging framework. A weighed imaging functional is defined using the concept of a weighted Helmholtz decomposition, initially proposed in [4] for time-reversal imaging of extended elastic sources. It is proved that the modified detection algorithm provides a resolution limit of the order of half a wavelength, indeed, as the new functional behaves as the square of the imaginary part of a pressure or shear Green function (cf. section 4.2). For simplicity, we restrict ourselves to the study of two particular situations when we have only a density contrast or an elasticity contrast. In order to cater to various applications, we provide explicit results for the canonical

cases of circular and spherical inclusions. It is also important to note that the formulae of the TD based functionals are explicit in terms of the incident wave and the free space fundamental solution instead of the Green function in the bounded domain with imposed boundary conditions. This is in contrast with the prior results; see, for instance, [19]. Albeit a Neumann boundary condition is imposed on the displacement field, the results of this paper extend to the problem with Dirichlet boundary conditions. A stability analysis of the TD based imaging functionals was also missing in the literature. In this paper we carry out a detailed stability analysis of the proposed imaging functionals with respect to both measurement and medium noises.

The rest of this paper is organized as follows: In section 2, we introduce some notation and present the asymptotic expansions due to the perturbation of the displacement field in the presence of small inclusions. Section 3 is devoted to the study of a TD imaging functional resulting from the expansion of the filtered quadratic misfit with respect to the size of the inclusion. As discussed in section 3.2, the resolution in the TD imaging framework is not optimal. Therefore, a modified imaging framework is established in section 4. The sensitivity analysis of the modified framework is presented in section 4.2. Sections 5 and 6 are devoted to the stability analysis with respect to measurement and medium noises, respectively. The paper is concluded in section 7.

2. Mathematical formulation. This section is devoted to preliminaries, notation, and assumptions used in the rest of this paper. We also recall a few fundamental results related to small volume asymptotic expansions of the displacement field due to the presence of a penetrable inclusion with respect to the size of the inclusion, which will be essential in what follows.

2.1. Preliminaries and notation. Consider a homogeneous isotropic elastic material occupying a bounded domain $\Omega \subset \mathbb{R}^d$ for $d = 2$ or 3 , with connected Lipschitz boundary $\partial\Omega$. Let the Lamé (compressional and shear) parameters of Ω be λ_0 and μ_0 , respectively, in the absence of any inclusion, and let $\rho_0 > 0$ be the (constant) volume density of the background. Let $D \subset \Omega$ be an elastic inclusion with Lamé parameters λ_1 , μ_1 and density $\rho_1 > 0$. Suppose that D is given by

$$(2.1) \quad D := \delta B + \mathbf{z}_a,$$

where B is a bounded Lipschitz domain in \mathbb{R}^d containing the origin and \mathbf{z}_a represents the location of the inclusion D . The small parameter δ represents the characteristic size of the diameter of D . Moreover, we assume that D is separated part from the boundary $\partial\Omega$; i.e., there exists a constant $c_0 > 0$ such that

$$(2.2) \quad \inf_{\mathbf{x} \in D} \text{dist}(\mathbf{x}, \partial\Omega) \geq c_0,$$

where dist denotes the distance. Further, it is assumed that

$$(2.3) \quad d\lambda_m + 2\mu_m > 0, \quad \mu_m > 0, \quad m \in \{0, 1\}, \quad (\lambda_0 - \lambda_1)(\mu_0 - \mu_1) \geq 0.$$

Consider the following transmission problem with the Neumann boundary condition:

$$(2.4) \quad \begin{cases} \mathcal{L}_{\lambda_0, \mu_0} \mathbf{u} + \rho_0 \omega^2 \mathbf{u} = 0 & \text{in } \Omega \setminus \overline{D}, \\ \mathcal{L}_{\lambda_1, \mu_1} \mathbf{u} + \rho_1 \omega^2 \mathbf{u} = 0 & \text{in } D, \\ \mathbf{u}|_- = \mathbf{u}|_+ & \text{on } \partial D, \\ \frac{\partial \mathbf{u}}{\partial \tilde{\nu}}|_- = \frac{\partial \mathbf{u}}{\partial \nu}|_+ & \text{on } \partial D, \\ \frac{\partial \mathbf{u}}{\partial \nu} = \mathbf{g} & \text{on } \partial \Omega, \end{cases}$$

where $\omega > 0$ is the angular frequency of the mechanical oscillations and the linear elasticity system $\mathcal{L}_{\lambda_0, \mu_0}$ and the conormal derivative $\frac{\partial}{\partial \tilde{\nu}}$, associated with parameters (λ_0, μ_0) , are defined by

$$(2.5) \quad \mathcal{L}_{\lambda_0, \mu_0}[\mathbf{w}] := \mu_0 \Delta \mathbf{w} + (\lambda_0 + \mu_0) \nabla \nabla \cdot \mathbf{w}$$

and

$$(2.6) \quad \frac{\partial \mathbf{w}}{\partial \tilde{\nu}} := \lambda_0 (\nabla \cdot \mathbf{w}) \mathbf{n} + \mu_0 (\nabla \mathbf{w}^T + (\nabla \mathbf{w}^T)^T) \mathbf{n},$$

respectively. Here superscript T indicates the transpose of a matrix, \mathbf{n} represents the outward unit normal to ∂D , and $\frac{\partial}{\partial \tilde{\nu}}$ is the conormal derivative associated with (λ_1, μ_1) . To ensure well-posedness, we assume that $\rho_0 \omega^2$ is different from the Neumann eigenvalues of the operator $-\mathcal{L}_{\lambda_0, \mu_0}$ in $(L^2(\Omega))^d$. Using the theory of collectively compact operators (see, for instance, [9, Appendix A.3]), one can show that for small δ the transmission problem (2.4) has a unique solution for any $\mathbf{g} \in (L^2(\partial \Omega))^d$.

Throughout this work, for a domain X , notations $|_-$ and $|_+$ indicate, respectively, the limits from inside and from outside X to its boundary ∂X , δ_{ij} represents the Kronecker's symbol, and

$$\alpha, \beta \in \{P, S\}, \quad i, j, k, l, i', j', k', l', p, q \in \{1, \dots, d\}, \quad m \in \{0, 1\},$$

where P and S stand for pressure and shear parts, respectively.

Statement of the problem. The problem under consideration is the following:

Given the displacement field \mathbf{u} , the solution of the Neumann problem (2.4) at the boundary $\partial \Omega$, identify the location \mathbf{z}_a of the inclusion D using a TD based sensitivity framework.

2.2. Asymptotic analysis and fundamental results. Consider the fundamental solution $\Gamma_m^\omega(\mathbf{x}, \mathbf{y}) := \Gamma_m^\omega(\mathbf{x} - \mathbf{y})$ of the homogeneous time-harmonic elastic wave equation in \mathbb{R}^d with parameters $(\lambda_m, \mu_m, \rho_m)$, i.e., the solution to

$$(2.7) \quad (\mathcal{L}_{\lambda_m, \mu_m} + \rho_m \omega^2) \Gamma_m^\omega(\mathbf{x} - \mathbf{y}) = \delta_{\mathbf{y}}(\mathbf{x}) \mathbf{I}_2 \quad \forall \mathbf{x} \in \mathbb{R}^d, \mathbf{x} \neq \mathbf{y},$$

subject to the Kupradze outgoing radiation conditions [23], where $\delta_{\mathbf{y}}$ is the Dirac mass at \mathbf{y} and \mathbf{I}_2 is the $d \times d$ identity matrix. Let $c_S = \sqrt{\frac{\mu_0}{\rho_0}}$ and $c_P = \sqrt{\frac{\lambda_0 + 2\mu_0}{\rho_0}}$ be the background shear

and the pressure wave speeds, respectively. Then $\mathbf{\Gamma}_0^\omega$ is given by [1]

$$(2.8) \quad \mathbf{\Gamma}_0^\omega(\mathbf{x}) = \left\{ \frac{1}{\mu_0} \mathbf{I}_2 G_S^\omega(\mathbf{x}) - \frac{1}{\rho_0 \omega^2} \mathbb{D}_{\mathbf{x}} [G_P^\omega(\mathbf{x}) - G_S^\omega(\mathbf{x})] \right\}, \quad \mathbf{x} \in \mathbb{R}^d, \quad d = 2, 3,$$

where the tensor $\mathbb{D}_{\mathbf{x}}$ is defined by

$$\mathbb{D}_{\mathbf{x}} = \nabla_{\mathbf{x}} \otimes \nabla_{\mathbf{x}} = (\partial_{ij})_{i,j=1}^d$$

and the function G_α^ω is the fundamental solution to the Helmholtz operator, i.e.,

$$(\Delta + \kappa_\alpha^2) G_\alpha^\omega(\mathbf{x}) = \delta_0(\mathbf{x}), \quad \mathbf{x} \in \mathbb{R}^d, \quad \mathbf{x} \neq \mathbf{0},$$

subject to the *Sommerfeld* outgoing radiation condition

$$\left| \frac{\partial G_\alpha^\omega}{\partial \mathbf{n}} - i \kappa_\alpha G_\alpha^\omega \right|(\mathbf{x}) = o(R^{1-d/2}), \quad \mathbf{x} \in \partial B(\mathbf{0}, R),$$

with $B(\mathbf{0}, R)$ being the sphere of radius R and center at the origin. Here $\partial_{ij} = \frac{\partial^2}{\partial x_i \partial x_j}$, $\kappa_\alpha := \frac{\omega}{c_\alpha}$ is the wave number, and $\frac{\partial}{\partial \mathbf{n}}$ represents the normal derivative.

The function G_α^ω is given by

$$(2.9) \quad G_\alpha^\omega(\mathbf{x}) = \begin{cases} -\frac{i}{4} H_0^{(1)}(\kappa_\alpha |\mathbf{x}|), & d = 2, \\ -\frac{e^{i \kappa_\alpha |\mathbf{x}|}}{4\pi |\mathbf{x}|}, & d = 3, \end{cases}$$

where $H_n^{(1)}$ is the order n Hankel function of first kind.

Note that $\mathbf{\Gamma}_0^\omega$ can be decomposed into shear and pressure components, i.e.,

$$(2.10) \quad \mathbf{\Gamma}_0^\omega(\mathbf{x}) = \mathbf{\Gamma}_{0,S}^\omega(\mathbf{x}) + \mathbf{\Gamma}_{0,P}^\omega(\mathbf{x}) \quad \forall \mathbf{x} \in \mathbb{R}^d, \quad \mathbf{x} \neq \mathbf{0},$$

where

$$(2.11) \quad \mathbf{\Gamma}_{0,P}^\omega(\mathbf{x}) = -\frac{1}{\mu_0 \kappa_S^2} \mathbb{D}_{\mathbf{x}} G_P^\omega(\mathbf{x}) \quad \text{and} \quad \mathbf{\Gamma}_{0,S}^\omega(\mathbf{x}) = \frac{1}{\mu_0 \kappa_S^2} (\kappa_S^2 \mathbf{I}_2 + \mathbb{D}_{\mathbf{x}}) G_S^\omega(\mathbf{x}).$$

Note that $\nabla \cdot \mathbf{\Gamma}_{0,S}^\omega = \mathbf{0}$ and $\nabla \times \mathbf{\Gamma}_{0,P}^\omega = \mathbf{0}$.

Let us define the single layer potential $\mathcal{S}_\Omega^\omega$ associated with $(\mathcal{L}_{\lambda_0, \mu_0} + \rho_0 \omega^2)$ by

$$(2.12) \quad \mathcal{S}_\Omega^\omega[\mathbf{\Phi}](\mathbf{x}) := \int_{\partial\Omega} \mathbf{\Gamma}_0^\omega(\mathbf{x} - \mathbf{y}) \mathbf{\Phi}(\mathbf{y}) d\sigma(\mathbf{y}), \quad \mathbf{x} \in \mathbb{R}^d,$$

and the boundary integral operator $\mathcal{K}_\Omega^\omega$ by

$$(2.13) \quad \mathcal{K}_\Omega^\omega[\mathbf{\Phi}](\mathbf{x}) := \text{p.v.} \int_{\partial\Omega} \frac{\partial}{\partial \nu_{\mathbf{y}}} \mathbf{\Gamma}_0^\omega(\mathbf{x} - \mathbf{y}) \mathbf{\Phi}(\mathbf{y}) d\sigma(\mathbf{y}) \quad \text{a.e. } \mathbf{x} \in \partial\Omega$$

for any function $\mathbf{\Phi} \in (L^2(\partial\Omega))^d$, where p.v. stands for Cauchy principal value.

Let $(\mathcal{K}_\Omega^\omega)^*$ be the adjoint operator of $\mathcal{K}_\Omega^{-\omega}$ on $(L^2(\partial\Omega))^d$, i.e.,

$$(\mathcal{K}_\Omega^\omega)^*[\Phi](\mathbf{x}) = \text{p.v.} \int_{\partial\Omega} \frac{\partial}{\partial\nu_{\mathbf{x}}} \Gamma_0^\omega(\mathbf{x} - \mathbf{y}) \Phi(\mathbf{y}) d\sigma(\mathbf{y}) \quad \text{a.e. } \mathbf{x} \in \partial\Omega.$$

It is well known (see, for instance, [2, section 3.4.3]) that the single layer potential, $\mathcal{S}_\Omega^\omega$, enjoys the following jump conditions:

$$(2.14) \quad \frac{\partial(\mathcal{S}_\Omega^\omega[\Phi])}{\partial\nu} \Big|_{\pm}(\mathbf{x}) = \left(\pm \frac{1}{2} I + (\mathcal{K}_\Omega^\omega)^* \right) [\Phi](\mathbf{x}) \quad \text{a.e. } \mathbf{x} \in \partial\Omega.$$

Let $\mathbf{N}^\omega(\mathbf{x}, \mathbf{y})$, for all $\mathbf{y} \in \Omega$, be the Neumann solution associated with $(\lambda_0, \mu_0, \rho_0)$ in Ω , i.e.,

$$(2.15) \quad \begin{cases} (\mathcal{L}_{\lambda_0, \mu_0} + \rho_0 \omega^2) \mathbf{N}^\omega(\mathbf{x}, \mathbf{y}) = -\delta_{\mathbf{y}}(\mathbf{x}) \mathbf{I}_2, & \mathbf{x} \in \Omega, \quad \mathbf{x} \neq \mathbf{y}, \\ \frac{\partial \mathbf{N}^\omega}{\partial\nu}(\mathbf{x}, \mathbf{y}) = 0, & \mathbf{x} \in \partial\Omega. \end{cases}$$

Then, by slightly modifying the proof for the case of zero frequency in [10], one can show that the following result holds.

Lemma 2.1. *For all $\mathbf{x} \in \partial\Omega$ and $\mathbf{y} \in \Omega$, we have*

$$(2.16) \quad \left(-\frac{1}{2} I + \mathcal{K}_\Omega^\omega \right) [\mathbf{N}^\omega(\cdot, \mathbf{y})](\mathbf{x}) = \Gamma_0^\omega(\mathbf{x} - \mathbf{y}),$$

where $\mathcal{K}_\Omega^\omega$ is defined by (2.13).

For $i, j \in \{1, \dots, d\}$, let \mathbf{v}_{ij} be the solution to

$$(2.17) \quad \begin{cases} \mathcal{L}_{\lambda_0, \mu_0} \mathbf{v}_{ij} = 0 & \text{in } \mathbb{R}^d \setminus \bar{B}, \\ \mathcal{L}_{\lambda_1, \mu_1} \mathbf{v}_{ij} = 0 & \text{in } B, \\ \mathbf{v}_{ij}|_- = \mathbf{v}_{ij}|_+ & \text{on } \partial B, \\ \frac{\partial \mathbf{v}_{ij}}{\partial \tilde{\nu}} \Big|_- = \frac{\partial \mathbf{v}_{ij}}{\partial \nu} \Big|_+ & \text{on } \partial B, \\ \mathbf{v}_{ij}(\mathbf{x}) - x_i \mathbf{e}_j = O(|\mathbf{x}|^{1-d}) & \text{as } |\mathbf{x}| \rightarrow \infty, \end{cases}$$

where $(\mathbf{e}_1, \dots, \mathbf{e}_d)$ denotes the standard basis for \mathbb{R}^d . Then the elastic moment tensor (EMT) $\mathbb{M} := (m_{ijpq})_{i,j,p,q=1}^d$ associated with domain B and the Lamé parameters $(\lambda_0, \mu_0; \lambda_1, \mu_1)$ is defined by

$$(2.18) \quad m_{ijpq} = \int_{\partial B} \left[\frac{\partial(x_p \mathbf{e}_q)}{\partial \tilde{\nu}} - \frac{\partial(x_p \mathbf{e}_q)}{\partial \nu} \right] \cdot \mathbf{v}_{ij} d\sigma;$$

see [10, 12]. In particular, for a circular or a spherical inclusion, \mathbb{M} can be expressed as

$$(2.19) \quad \mathbb{M} = a \mathbb{I}_4 + b \mathbf{I}_2 \otimes \mathbf{I}_2$$

or, equivalently, as

$$m_{ijkl} = \frac{a}{2}(\delta_{ik}\delta_{jl} + \delta_{il}\delta_{jk}) + b\delta_{ij}\delta_{kl}$$

for some constants a and b depending only on $\lambda_0, \lambda_1, \mu_0, \mu_1$ and the space dimension d [2, section 7.3.2]. Here \mathbb{I}_4 is the identity 4-tensor. Note that for any $d \times d$ symmetric matrix \mathbf{A} , $\mathbb{I}_4(\mathbf{A}) = \mathbf{A}$. Furthermore, throughout this paper we make the assumption that $\mu_1 \geq \mu_0$ and $\lambda_1 \geq \lambda_0$ in order to ensure that the constants a and b are positive.

It is known that the EMT \mathbb{M} has the following symmetry property:

$$(2.20) \quad m_{ijpq} = m_{pqij} = m_{jipq} = m_{ijqp},$$

which allows us to identify \mathbb{M} with a symmetric linear transformation on the space of symmetric $d \times d$ matrices. It also satisfies the positivity property (positive or negative definiteness) on the space of symmetric matrices [10, 12].

Let \mathbf{U} be the background solution associated with $(\lambda_0, \mu_0, \rho_0)$ in Ω , i.e.,

$$(2.21) \quad \begin{cases} (\mathcal{L}_{\lambda_0, \mu_0} + \rho_0 \omega^2) \mathbf{U} = 0 & \text{on } \Omega, \\ \frac{\partial \mathbf{U}}{\partial \nu} = \mathbf{g} & \text{on } \partial\Omega. \end{cases}$$

Then, the following result can be obtained using arguments analogous to those in [8, 10]; see [5]. Here and throughout this paper

$$\mathbf{A} : \mathbf{B} = \sum_{i,j=1}^d a_{ij} b_{ij}$$

for matrices $\mathbf{A} = (a_{ij})_{i,j=1}^d$ and $\mathbf{B} = (b_{ij})_{i,j=1}^d$.

Theorem 2.2. *Let \mathbf{u} be the solution to (2.4), \mathbf{U} be the background solution defined by (2.21), and $\rho_0 \omega^2$ be different from the Neumann eigenvalues of the operator $-\mathcal{L}_{\lambda_0, \mu_0}$ in $(L^2(\Omega))^d$. Let D be given by (2.1), and let conditions (2.2) and (2.3) be satisfied. Then, for $\omega \delta \ll 1$, the following asymptotic expansion holds uniformly for all $\mathbf{x} \in \partial\Omega$:*

$$(2.22) \quad \mathbf{u}(\mathbf{x}) - \mathbf{U}(\mathbf{x}) = -\delta^d \left(\nabla \mathbf{U}(\mathbf{z}_a) : \mathbb{M}(B) \nabla_{\mathbf{z}_a} \mathbf{N}^\omega(\mathbf{x}, \mathbf{z}_a) \right. \\ \left. + \omega^2 (\rho_0 - \rho_1) |B| \mathbf{N}^\omega(\mathbf{x}, \mathbf{z}_a) \mathbf{U}(\mathbf{z}_a) \right) + O(\delta^{d+1}).$$

As a direct consequence of expansion (2.22) and Lemma 2.1, the following result holds.

Corollary 2.3. *Under the assumptions of Theorem 2.2, we have*

$$(2.23) \quad \left(\frac{1}{2} I - \mathcal{K}_\Omega^\omega \right) [\mathbf{u} - \mathbf{U}](\mathbf{x}) \\ = \delta^d \left(\nabla \mathbf{U}(\mathbf{z}_a) : \mathbb{M}(B) \nabla_{\mathbf{z}_a} \mathbf{\Gamma}_0^\omega(\mathbf{x} - \mathbf{z}_a) + \omega^2 (\rho_0 - \rho_1) |B| \mathbf{\Gamma}_0^\omega(\mathbf{x} - \mathbf{z}_a) \mathbf{U}(\mathbf{z}_a) \right) + O(\delta^{d+1})$$

uniformly with respect to $\mathbf{x} \in \partial\Omega$.

Remark 2.4. We have made use of the following conventions in (2.22) and (2.23):

$$\left(\nabla\mathbf{U}(\mathbf{z}_a) : \mathbb{M}(B)\nabla_{\mathbf{z}_a}\mathbf{N}^\omega(\mathbf{x}, \mathbf{z}_a)\right)_k = \sum_{i,j=1}^d \left(\partial_i\mathbf{U}_j(\mathbf{z}_a) \sum_{p,q=1}^d m_{ijpq}\partial_p\mathbf{N}_{kq}^\omega(\mathbf{x}, \mathbf{z}_a)\right)$$

and

$$\left(\mathbf{N}^\omega(\mathbf{x}, \mathbf{z}_a)\mathbf{U}(\mathbf{z}_a)\right)_k = \sum_{i=1}^d \mathbf{N}_{ki}^\omega(\mathbf{x}, \mathbf{z}_a)\mathbf{U}_i(\mathbf{z}_a).$$

3. Imaging small inclusions using TD. In this section, we consider a filtered quadratic misfit and introduce a TD based imaging functional resulting therefrom and analyze its performance when identifying true location \mathbf{z}_a of the inclusion D .

For a search point \mathbf{z}^S , let $\mathbf{u}_{\mathbf{z}^S}$ be the solution to (2.4) in the presence of a trial inclusion $D' = \delta'B' + \mathbf{z}^S$ with parameters $(\lambda'_1, \mu'_1, \rho'_1)$, where B' is chosen a priori and δ' is small. Assume that

$$(3.1) \quad d\lambda'_1 + 2\mu'_1 > 0, \quad \mu'_1 > 0, \quad (\lambda_0 - \lambda'_1)(\mu_0 - \mu'_1) \geq 0.$$

Consider the elastic counterpart of the filtered quadratic misfit proposed by Ammari et al. in [6], that is, the following misfit:

$$(3.2) \quad \mathcal{E}_f[\mathbf{U}](\mathbf{z}^S) = \frac{1}{2} \int_{\partial\Omega} \left| \left(\frac{1}{2}I - \mathcal{K}_\Omega^\omega \right) [\mathbf{u}_{\mathbf{z}^S} - \mathbf{u}_{\text{meas}}](\mathbf{x}) \right|^2 d\sigma(\mathbf{x}).$$

As shown for Helmholtz equations in [6], the identification of the exact location of true inclusion using the classical quadratic misfit

$$(3.3) \quad \mathcal{E}[\mathbf{U}](\mathbf{z}^S) = \frac{1}{2} \int_{\partial\Omega} |(\mathbf{u}_{\mathbf{z}^S} - \mathbf{u}_{\text{meas}})(\mathbf{x})|^2 d\sigma(\mathbf{x})$$

cannot be guaranteed, and the postprocessing of the data is necessary. We show in the later part of this section that exact identification can be achieved using filtered quadratic misfit \mathcal{E}_f .

We emphasize that the postprocessing compensates for the effects of an imposed Neumann boundary condition on the displacement field.

3.1. TD of the filtered quadratic misfit. Analogously to Theorem 2.2, the displacement field $\mathbf{u}_{\mathbf{z}^S}$, in the presence of the trial inclusion at the search location, can be expanded as

$$(3.4) \quad \begin{aligned} \mathbf{u}_{\mathbf{z}^S}(x) - \mathbf{U}(\mathbf{x}) = & -(\delta')^d \left(\nabla\mathbf{U}(\mathbf{z}^S) : \mathbb{M}'(B')\nabla_{\mathbf{z}^S}\mathbf{N}^\omega(\mathbf{x}, \mathbf{z}^S) \right. \\ & \left. + \omega^2(\rho_0 - \rho'_1)|B'|\mathbf{N}^\omega(\mathbf{x}, \mathbf{z}^S)\mathbf{U}(\mathbf{z}^S) \right) + O\left((\delta')^{d+1}\right) \end{aligned}$$

for a small $\delta' > 0$, where $\mathbb{M}'(B')$ is the EMT associated with the domain B' and the parameters $(\lambda_0, \mu_0; \lambda'_1, \mu'_1)$. Following the arguments in [6], we obtain, by using Corollary 2.3 and the jump

conditions (2.14), that

$$\begin{aligned}
 \mathcal{E}_f[\mathbf{U}](\mathbf{z}^S) &= \frac{1}{2} \int_{\partial\Omega} \left| \left(\frac{1}{2}I - \mathcal{K}_\Omega^\omega \right) [\mathbf{U} - \mathbf{u}_{\text{meas}}](\mathbf{x}) \right|^2 d\sigma(\mathbf{x}) \\
 &\quad + (\delta')^d \Re e \left\{ \nabla \mathbf{U}(\mathbf{z}^S) : \mathbb{M}'(B') \nabla \mathbf{w}(\mathbf{z}^S) + \omega^2 (\rho_0 - \rho'_1) |B'| \mathbf{U}(\mathbf{z}^S) \cdot \mathbf{w}(\mathbf{z}^S) \right\} \\
 (3.5) \quad &\quad + O\left((\delta\delta')^d\right) + O\left((\delta')^{2d}\right),
 \end{aligned}$$

where the function \mathbf{w} is defined in terms of the measured data $(\mathbf{U} - \mathbf{u}_{\text{meas}})$ by

$$(3.6) \quad \mathbf{w}(\mathbf{x}) = \mathcal{S}_\Omega^\omega \left[\overline{\left(\frac{1}{2}I - \mathcal{K}_\Omega^\omega \right) [\mathbf{u}_{\text{meas}} - \mathbf{U}]} \right](\mathbf{x}), \quad \mathbf{x} \in \Omega.$$

The function \mathbf{w} corresponds to backpropagating inside Ω the boundary measurements of $\mathbf{U} - \mathbf{u}_{\text{meas}}$. Substituting (2.23) in (3.6), we find that

$$\begin{aligned}
 \mathbf{w}(\mathbf{z}^S) &= \delta^d \left(\nabla \overline{\mathbf{U}}(\mathbf{z}_a) : \mathbb{M}(B) \left[\int_{\partial\Omega} \Gamma_0^\omega(\mathbf{z}^S - \mathbf{x}) \nabla_{\mathbf{z}_a} \overline{\Gamma_0^\omega}(\mathbf{x} - \mathbf{z}_a) d\sigma(\mathbf{x}) \right] \right. \\
 (3.7) \quad &\quad \left. + \omega^2 (\rho_0 - \rho_1) |B| \left[\int_{\partial\Omega} \overline{\Gamma_0^\omega}(\mathbf{x} - \mathbf{z}_a) \Gamma_0^\omega(\mathbf{x} - \mathbf{z}^S) d\sigma(\mathbf{x}) \right] \overline{\mathbf{U}}(\mathbf{z}_a) \right) + O(\delta^{d+1}).
 \end{aligned}$$

Definition 3.1 (TD of \mathcal{E}_f). The TD imaging functional associated with \mathcal{E}_f at a search point $\mathbf{z}^S \in \Omega$ is defined by

$$(3.8) \quad \mathcal{I}_{\text{TD}}[\mathbf{U}](\mathbf{z}^S) := - \left. \frac{\partial \mathcal{E}_f[\mathbf{U}](\mathbf{z}^S)}{\partial (\delta')^d} \right|_{(\delta')^d=0}.$$

Note that from (3.5) it follows that

$$(3.9) \quad \mathcal{I}_{\text{TD}}[\mathbf{U}](\mathbf{z}^S) = - \Re e \left\{ \nabla \mathbf{U}(\mathbf{z}^S) : \mathbb{M}'(B') \nabla \mathbf{w}(\mathbf{z}^S) + \omega^2 (\rho_0 - \rho'_1) |B'| \mathbf{U}(\mathbf{z}^S) \cdot \mathbf{w}(\mathbf{z}^S) \right\},$$

where \mathbf{w} is given by (3.7).

The functional $\mathcal{I}_{\text{TD}}[\mathbf{U}](\mathbf{z}^S)$ at every search point $\mathbf{z}^S \in \Omega$ synthesizes the sensitivity of the misfit \mathcal{E}_f relative to the insertion of an elastic inclusion $D' = \mathbf{z}^S + \delta' B'$ at that point. The maximum of $\mathcal{I}_{\text{TD}}[\mathbf{U}](\mathbf{z}^S)$ corresponds to the point at which the insertion of an inclusion centered at that point maximally decreases the misfit \mathcal{E}_f . For Helmholtz equations, as shown in [6], the location of the maximum of $\mathcal{I}_{\text{TD}}[\mathbf{U}](\mathbf{z}^S)$ is a good estimate of the location \mathbf{z}_a of the true inclusion, D , that determines the measured field. In the next section, we explain why TD imaging functional \mathcal{I}_{TD} , defined by (3.8), may not attain its maximum at the location \mathbf{z}_a of the true inclusion.

3.2. Sensitivity analysis of TD. We first notice that the functional \mathcal{I}_{TD} consists of two terms: a density contrast term and an elasticity contrast term with background material. For simplicity and purely for analysis sake, we consider two special cases when we have only the density contrast or the elasticity contrast with reference medium.

3.2.1. Case I: Density contrast. Suppose that $\lambda_0 = \lambda_1$ and $\mu_0 = \mu_1$. In this case, the wave function \mathbf{w} satisfies

$$(3.10) \quad \mathbf{w}(\mathbf{z}^S) \simeq \delta^d \left(\omega^2(\rho_0 - \rho_1)|B| \left[\int_{\partial\Omega} \overline{\Gamma_0^\omega(\mathbf{x} - \mathbf{z}_a)} \Gamma_0^\omega(\mathbf{x} - \mathbf{z}^S) d\sigma(\mathbf{x}) \right] \overline{\mathbf{U}}(\mathbf{z}_a) \right).$$

Consequently, the imaging functional \mathcal{I}_{TD} at $\mathbf{z}^S \in \Omega$ reduces to

$$(3.11) \quad \mathcal{I}_{\text{TD}}[\mathbf{U}](\mathbf{z}^S) \simeq C \omega^4 \Re e \left\{ \mathbf{U}(\mathbf{z}^S) \cdot \left[\left(\int_{\partial\Omega} \overline{\Gamma_0^\omega(\mathbf{x} - \mathbf{z}_a)} \Gamma_0^\omega(\mathbf{x} - \mathbf{z}^S) d\sigma(\mathbf{x}) \right) \overline{\mathbf{U}}(\mathbf{z}_a) \right] \right\},$$

where

$$(3.12) \quad C = \delta^d(\rho_0 - \rho'_1)(\rho_0 - \rho_1)|B'| |B|.$$

Throughout this paper we assume that

$$(\rho_0 - \rho'_1)(\rho_0 - \rho_1) \geq 0.$$

Let us recall the following estimates from [4, Proposition 2.5], which hold as the distance between the points \mathbf{z}^S and \mathbf{z}_a and the boundary $\partial\Omega$ goes to infinity.

Lemma 3.2 (Helmholtz–Kirchhoff identities). *For $\mathbf{z}^S, \mathbf{z}_a \in \Omega$ far from the boundary $\partial\Omega$, compared to the wavelength of the wave impinging upon Ω , we have*

$$\begin{aligned} \int_{\partial\Omega} \overline{\Gamma_{0,\alpha}^\omega(\mathbf{x} - \mathbf{z}_a)} \Gamma_{0,\alpha}^\omega(\mathbf{x} - \mathbf{z}^S) d\sigma(\mathbf{x}) &\simeq -\frac{1}{c_\alpha \omega} \Im m \left\{ \Gamma_{0,\alpha}^\omega(\mathbf{z}^S - \mathbf{z}_a) \right\}, \\ \int_{\partial\Omega} \overline{\Gamma_{0,\alpha}^\omega(\mathbf{x} - \mathbf{z}_a)} \Gamma_{0,\beta}^\omega(\mathbf{x} - \mathbf{z}^S) d\sigma(\mathbf{x}) &\simeq 0, \quad \alpha \neq \beta. \end{aligned}$$

Therefore, by virtue of (2.10) and Lemma 3.2, we can easily get

$$(3.13) \quad \mathcal{I}_{\text{TD}}[\mathbf{U}](\mathbf{z}^S) \simeq -C \omega^3 \Re e \left\{ \mathbf{U}(\mathbf{z}^S) \cdot \left[\Im m \left\{ \frac{1}{c_P} \Gamma_{0,P}^\omega(\mathbf{z}^S - \mathbf{z}_a) + \frac{1}{c_S} \Gamma_{0,S}^\omega(\mathbf{z}^S - \mathbf{z}_a) \right\} \overline{\mathbf{U}}(\mathbf{z}_a) \right] \right\}.$$

Let $(\mathbf{e}_{\theta_1}, \mathbf{e}_{\theta_2}, \dots, \mathbf{e}_{\theta_n})$ be n uniformly distributed directions over the unit disk or sphere, and denote by \mathbf{U}_j^P and \mathbf{U}_j^S , respectively, the P -plane and S -plane waves, that is,

$$(3.14) \quad \mathbf{U}_j^P(\mathbf{x}) = e^{i\kappa_P \mathbf{x} \cdot \mathbf{e}_{\theta_j}} \mathbf{e}_{\theta_j} \quad \text{and} \quad \mathbf{U}_j^S(\mathbf{x}) = e^{i\kappa_S \mathbf{x} \cdot \mathbf{e}_{\theta_j}} \mathbf{e}_{\theta_j}^\perp$$

for $d = 2$. In three dimensions, we set

$$\mathbf{U}_{j,l}^S(\mathbf{x}) = e^{i\kappa_S \mathbf{x} \cdot \mathbf{e}_{\theta_j}} \mathbf{e}_{\theta_j}^{\perp,l}, \quad l = 1, 2,$$

where $(\mathbf{e}_{\theta_j}, \mathbf{e}_{\theta_j}^{\perp,1}, \mathbf{e}_{\theta_j}^{\perp,2})$ is an orthonormal basis of \mathbb{R}^3 . For ease of notation, in three dimensions, $\mathcal{I}_{\text{TD}}[\mathbf{U}_j^S](\mathbf{z}^S)$ denotes $\sum_{l=1}^2 \mathcal{I}_{\text{TD}}[\mathbf{U}_{j,l}^S](\mathbf{z}^S)$.

We have

$$(3.15) \quad \frac{1}{n} \sum_{j=1}^n e^{i\kappa_\alpha \mathbf{x} \cdot \mathbf{e}_{\theta_j}} \simeq -4 \left(\frac{\pi}{\kappa_\alpha} \right)^{d-2} \Im m G_\alpha^\omega(\mathbf{x})$$

for large n ; see, for instance, [6]. The following proposition holds.

Proposition 3.3. *Let \mathbf{U}_j^α be defined in (3.14), where $j = 1, 2, \dots, n$, for n sufficiently large. Then, for all $\mathbf{z}^S \in \Omega$ far from $\partial\Omega$,*

$$(3.16) \quad \frac{1}{n} \sum_{j=1}^n \mathcal{I}_{\text{TD}}[\mathbf{U}_j^P](\mathbf{z}^S) \simeq 4\mu_0 C \omega^3 \left(\frac{\pi}{\kappa_P} \right)^{d-2} \left(\frac{\kappa_S}{\kappa_P} \right)^2 \left[\frac{1}{C_P} |\Im m \{ \Gamma_{0,P}^\omega(\mathbf{z}^S - \mathbf{z}_a) \}|^2 + \frac{1}{C_S} \Im m \{ \Gamma_{0,P}^\omega(\mathbf{z}^S - \mathbf{z}_a) \} : \Im m \{ \Gamma_{0,S}^\omega(\mathbf{z}^S - \mathbf{z}_a) \} \right],$$

and

$$(3.17) \quad \frac{1}{n} \sum_{j=1}^n \mathcal{I}_{\text{TD}}[\mathbf{U}_j^S](\mathbf{z}^S) \simeq 4\mu_0 C \omega^3 \left(\frac{\pi}{\kappa_S} \right)^{d-2} \left[\frac{1}{C_S} |\Im m \{ \Gamma_{0,S}^\omega(\mathbf{z}^S - \mathbf{z}_a) \}|^2 + \frac{1}{C_P} \Im m \{ \Gamma_{0,P}^\omega(\mathbf{z}^S - \mathbf{z}_a) \} : \Im m \{ \Gamma_{0,S}^\omega(\mathbf{z}^S - \mathbf{z}_a) \} \right],$$

where C is given by (3.12).

Proof. From (3.15) it follows that

$$(3.18) \quad \begin{aligned} \frac{1}{n} \sum_{j=1}^n e^{i\kappa_P \mathbf{x} \cdot \mathbf{e}_{\theta_j}} \mathbf{e}_{\theta_j} \otimes \mathbf{e}_{\theta_j} &\simeq 4 \left(\frac{\pi}{\kappa_P} \right)^{d-2} \Im m \left\{ \frac{1}{\kappa_P^2} \mathbb{D}_{\mathbf{x}} G_P^\omega(\mathbf{x}) \right\} \\ &\simeq -4\mu_0 \left(\frac{\pi}{\kappa_P} \right)^{d-2} \left(\frac{\kappa_S}{\kappa_P} \right)^2 \Im m \{ \Gamma_{0,P}^\omega(\mathbf{x}) \} \end{aligned}$$

and

$$(3.19) \quad \begin{aligned} \frac{1}{n} \sum_{j=1}^n e^{i\kappa_S \mathbf{x} \cdot \mathbf{e}_{\theta_j}} \mathbf{e}_{\theta_j}^\perp \otimes \mathbf{e}_{\theta_j}^\perp &= \frac{1}{n} \sum_{j=1}^n e^{i\kappa_S \mathbf{x} \cdot \mathbf{e}_{\theta_j}} (\mathbf{I}_2 - \mathbf{e}_{\theta_j} \otimes \mathbf{e}_{\theta_j}) \\ &\simeq -4 \left(\frac{\pi}{\kappa_S} \right)^{d-2} \Im m \left\{ \left(\mathbf{I}_2 + \frac{1}{\kappa_S^2} \mathbb{D}_{\mathbf{x}} \right) G_S^\omega(\mathbf{x}) \right\} \\ &= -4\mu_0 \left(\frac{\pi}{\kappa_S} \right)^{d-2} \Im m \{ \Gamma_{0,S}^\omega(\mathbf{x}) \}, \end{aligned}$$

where the last equality comes from (2.11). Note that, in three dimensions, (3.19) is to be understood as follows:

$$(3.20) \quad \frac{1}{n} \sum_{j=1}^n \sum_{l=1}^2 e^{i\kappa_S \mathbf{x} \cdot \mathbf{e}_{\theta_j}} \mathbf{e}_{\theta_j}^{\perp,l} \otimes \mathbf{e}_{\theta_j}^{\perp,l} \simeq -4\mu_0 \left(\frac{\pi}{\kappa_S} \right) \Im m \{ \Gamma_{0,S}^\omega(\mathbf{x}) \}.$$

Then, using the definition of \mathbf{U}_j^P we compute imaging functional \mathcal{I}_{TD} for n P -plane waves as

$$\begin{aligned} \frac{1}{n} \sum_{j=1}^n \mathcal{I}_{\text{TD}}[\mathbf{U}_j^P](\mathbf{z}^S) &= C\omega^4 \frac{1}{n} \sum_{j=1}^n \Re e \mathbf{U}_j^P(\mathbf{z}^S) \cdot \left[\int_{\partial\Omega} \overline{\Gamma_0^\omega}(\mathbf{x} - \mathbf{z}_a) \Gamma_0^\omega(\mathbf{x} - \mathbf{z}^S) d\sigma(\mathbf{x}) \overline{\mathbf{U}_j^P}(\mathbf{z}_a) \right] \\ &\simeq -C\omega^3 \frac{1}{n} \sum_{j=1}^n \Re e e^{i\kappa_P(\mathbf{z}^S - \mathbf{z}_a) \cdot \mathbf{e}_{\theta_j}} \mathbf{e}_{\theta_j} \cdot \left[\Im m \left\{ \frac{1}{c_P} \Gamma_{0,P}^\omega(\mathbf{z}^S - \mathbf{z}_a) \right. \right. \\ &\qquad \qquad \qquad \left. \left. + \frac{1}{c_S} \Gamma_{0,S}^\omega(\mathbf{z}^S - \mathbf{z}_a) \right\} \mathbf{e}_{\theta_j} \right] \\ &\simeq -C\omega^3 \Re e \left[\frac{1}{n} \sum_{j=1}^n e^{i\kappa_P(\mathbf{z}^S - \mathbf{z}_a) \cdot \mathbf{e}_{\theta_j}} \mathbf{e}_{\theta_j} \otimes \mathbf{e}_{\theta_j} \right] \\ &\qquad \qquad \qquad : \left[\Im m \left\{ \frac{1}{c_P} \Gamma_{0,P}^\omega(\mathbf{z}^S - \mathbf{z}_a) + \frac{1}{c_S} \Gamma_{0,S}^\omega(\mathbf{z}^S - \mathbf{z}_a) \right\} \right]. \end{aligned}$$

Here we used the fact that $\mathbf{e}_{\theta_j} \cdot \mathbf{A} \mathbf{e}_{\theta_j} = \mathbf{e}_{\theta_j} \otimes \mathbf{e}_{\theta_j} : \mathbf{A}$ for a matrix \mathbf{A} , which is easy to check.

Finally, exploiting the approximation (3.18), we conclude that

$$\begin{aligned} \frac{1}{n} \sum_{j=1}^n \mathcal{I}_{\text{TD}}[\mathbf{U}_j^P](\mathbf{z}^S) &\simeq 4\mu_0 C\omega^3 \left(\frac{\pi}{\kappa_P} \right)^{d-2} \left(\frac{\kappa_S}{\kappa_P} \right)^2 \left[\frac{1}{c_P} |\Im m \{ \Gamma_{0,P}^\omega(\mathbf{z}^S - \mathbf{z}_a) \}|^2 \right. \\ &\qquad \qquad \qquad \left. + \frac{1}{c_S} \Im m \{ \Gamma_{0,P}^\omega(\mathbf{z}^S - \mathbf{z}_a) \} : \Im m \{ \Gamma_{0,S}^\omega(\mathbf{z}^S - \mathbf{z}_a) \} \right]. \end{aligned}$$

Similarly, we can compute the imaging functional \mathcal{I}_{TD} for n S -plane waves exploiting the approximation (3.19) as

$$\begin{aligned} \frac{1}{n} \sum_{j=1}^n \mathcal{I}_{\text{TD}}[\mathbf{U}_j^S](\mathbf{z}^S) &= C\omega^4 \frac{1}{n} \sum_{j=1}^n \Re e \mathbf{U}_j^S(\mathbf{z}^S) \cdot \left[\int_{\partial\Omega} \overline{\Gamma_0^\omega}(\mathbf{x} - \mathbf{z}_a) \Gamma_0^\omega(\mathbf{x} - \mathbf{z}^S) d\sigma(\mathbf{x}) \overline{\mathbf{U}_j^S}(\mathbf{z}_a) \right] \\ &\simeq -C\omega^3 \frac{1}{n} \sum_{j=1}^n \Re e e^{i\kappa_S(\mathbf{z}^S - \mathbf{z}_a) \cdot \mathbf{e}_{\theta_j}} \mathbf{e}_{\theta_j}^\perp \cdot \left[\Im m \left\{ \frac{1}{c_P} \Gamma_{0,P}^\omega(\mathbf{z}^S - \mathbf{z}_a) \right. \right. \\ &\qquad \qquad \qquad \left. \left. + \frac{1}{c_S} \Gamma_{0,S}^\omega(\mathbf{z}^S - \mathbf{z}_a) \right\} \mathbf{e}_{\theta_j}^\perp \right] \\ &\simeq -C\omega^3 \Re e \left[\frac{1}{n} \sum_{j=1}^n e^{i\kappa_S(\mathbf{z}^S - \mathbf{z}_a) \cdot \mathbf{e}_{\theta_j}} \mathbf{e}_{\theta_j}^\perp \otimes \mathbf{e}_{\theta_j}^\perp \right] \\ &\qquad \qquad \qquad : \left[\Im m \left\{ \frac{1}{c_P} \Gamma_{0,P}^\omega(\mathbf{z}^S - \mathbf{z}_a) + \frac{1}{c_S} \Gamma_{0,S}^\omega(\mathbf{z}^S - \mathbf{z}_a) \right\} \right] \end{aligned}$$

$$\begin{aligned} &\simeq 4\mu_0 C\omega^3 \left(\frac{\pi}{\kappa_S}\right)^{d-2} \left[\frac{1}{c_S} |\Im m \{ \mathbf{\Gamma}_{0,S}^\omega(\mathbf{z}^S - \mathbf{z}_a) \}|^2 \right. \\ &\quad \left. + \frac{1}{c_P} \Im m \{ \mathbf{\Gamma}_{0,P}^\omega(\mathbf{z}^S - \mathbf{z}_a) \} : \Im m \{ \mathbf{\Gamma}_{0,S}^\omega(\mathbf{z}^S - \mathbf{z}_a) \} \right]. \end{aligned}$$

In dimension 3, one should use (3.20) to get the desired result. This completes the proof. ■

From Proposition 3.3, it is not clear that the imaging functional \mathcal{I}_{TD} attains its maximum at \mathbf{z}_a . Moreover, for both $\frac{1}{n} \sum_{j=1}^n \mathcal{I}_{TD}[\mathbf{U}_j^S](\mathbf{z}^S)$ and $\frac{1}{n} \sum_{j=1}^n \mathcal{I}_{TD}[\mathbf{U}_j^P](\mathbf{z}^S)$, the resolution at \mathbf{z}_a is not fine enough due to the presence of the term $\Im m \{ \mathbf{\Gamma}_{0,P}^\omega(\mathbf{z}^S - \mathbf{z}_a) \} : \Im m \{ \mathbf{\Gamma}_{0,S}^\omega(\mathbf{z}^S - \mathbf{z}_a) \}$. One way to cancel out this term is to combine $\frac{1}{n} \sum_{j=1}^n \mathcal{I}_{TD}[\mathbf{U}_j^S](\mathbf{z}^S)$ and $\frac{1}{n} \sum_{j=1}^n \mathcal{I}_{TD}[\mathbf{U}_j^P](\mathbf{z}^S)$ as follows:

$$\frac{1}{n} \sum_{j=1}^n \left(c_S \left(\frac{\kappa_P}{\pi}\right)^{d-2} \left(\frac{\kappa_P}{\kappa_S}\right)^2 \mathcal{I}_{TD}[\mathbf{U}_j^P](\mathbf{z}^S) - c_P \left(\frac{\kappa_S}{\pi}\right)^{d-2} \mathcal{I}_{TD}[\mathbf{U}_j^S](\mathbf{z}^S) \right).$$

However, one arrives at

$$\begin{aligned} &\frac{1}{n} \sum_{j=1}^n \left(c_S \left(\frac{\kappa_P}{\pi}\right)^{d-2} \left(\frac{\kappa_P}{\kappa_S}\right)^2 \mathcal{I}_{TD}[\mathbf{U}_j^P](\mathbf{z}^S) - c_P \left(\frac{\kappa_S}{\pi}\right)^{d-2} \mathcal{I}_{TD}[\mathbf{U}_j^S](\mathbf{z}^S) \right) \\ &\simeq 4\mu_0 C\omega^3 \left(\frac{c_S}{c_P} |\Im m \{ \mathbf{\Gamma}_{0,P}^\omega(\mathbf{z}^S - \mathbf{z}_a) \}|^2 - \frac{c_P}{c_S} |\Im m \{ \mathbf{\Gamma}_{0,S}^\omega(\mathbf{z}^S - \mathbf{z}_a) \}|^2 \right), \end{aligned}$$

which is not a sum of positive terms and thus cannot guarantee that the maximum of the obtained imaging functional is at the location of the inclusion.

3.2.2. Case II: Elasticity contrast. Suppose $\rho_0 = \rho_1$. Further, we assume for simplicity that $\mathbb{M} = \mathbb{M}'(B') = \mathbb{M}(B)$. From Lemma 3.2 we have

$$\begin{aligned} (3.21) \quad \int_{\partial\Omega} \nabla_{\mathbf{z}_a} \overline{\mathbf{\Gamma}}_0^\omega(\mathbf{x} - \mathbf{z}_a) \nabla_{\mathbf{z}^S} \mathbf{\Gamma}_0^\omega(\mathbf{x} - \mathbf{z}^S) d\sigma(\mathbf{x}) &\simeq -\frac{1}{c_S \omega} \Im m \{ \nabla_{\mathbf{z}_a} \nabla_{\mathbf{z}^S} \mathbf{\Gamma}_{0,S}^\omega(\mathbf{z}^S - \mathbf{z}_a) \} \\ &\quad - \frac{1}{c_P \omega} \Im m \{ \nabla_{\mathbf{z}_a} \nabla_{\mathbf{z}^S} \mathbf{\Gamma}_{0,P}^\omega(\mathbf{z}^S - \mathbf{z}_a) \}. \end{aligned}$$

Then, using (3.7) and (3.21), $\mathcal{I}_{TD}[\mathbf{U}](\mathbf{z}^S)$ at $\mathbf{z}^S \in \Omega$ becomes

$$\begin{aligned} (3.22) \quad \mathcal{I}_{TD}[\mathbf{U}](\mathbf{z}^S) &= -\delta^d \Re e \nabla \mathbf{U}(\mathbf{z}^S) : \mathbb{M} \nabla \mathbf{w}(\mathbf{z}^S) \\ &= \delta^d \Re e \nabla \mathbf{U}(\mathbf{z}^S) : \mathbb{M} \left[\int_{\partial\Omega} \nabla_{\mathbf{z}_a} \overline{\mathbf{\Gamma}}_0^\omega(\mathbf{x} - \mathbf{z}_a) \nabla_{\mathbf{z}^S} \mathbf{\Gamma}_0^\omega(\mathbf{x} - \mathbf{z}^S) d\sigma(\mathbf{x}) : \mathbb{M} \overline{\nabla \mathbf{U}}(\mathbf{z}_a) \right] \\ &\simeq \frac{\delta^d}{\omega} \Re e \nabla \mathbf{U}(\mathbf{z}^S) : \mathbb{M} \left[\nabla^2 \left(\Im m \{ \widetilde{\mathbf{\Gamma}}_0^\omega(\mathbf{z}^S - \mathbf{z}_a) \} \right) : \mathbb{M} \overline{\nabla \mathbf{U}}(\mathbf{z}_a) \right], \end{aligned}$$

where

$$(3.23) \quad \widetilde{\mathbf{\Gamma}}_0^\omega(\mathbf{z}^S - \mathbf{z}_a) = \frac{1}{c_P} \mathbf{\Gamma}_{0,P}^\omega(\mathbf{z}^S - \mathbf{z}_a) + \frac{1}{c_S} \mathbf{\Gamma}_{0,S}^\omega(\mathbf{z}^S - \mathbf{z}_a).$$

Let us define

$$(3.24) \quad J_{\alpha,\beta}(\mathbf{z}^S) := \left(\mathbb{M}\mathfrak{S}m \left[(\nabla^2 \Gamma_{0,\alpha}^\omega)(\mathbf{z}^S - \mathbf{z}_a) \right] \right) : \left(\mathbb{M}\mathfrak{S}m \left[(\nabla^2 \Gamma_{0,\beta}^\omega)(\mathbf{z}^S - \mathbf{z}_a) \right] \right)^T,$$

where $\mathbb{A}^T = (A_{klij})$ if \mathbb{A} is the 4-tensor given by $\mathbb{A} = (A_{ijkl})$. Here $\mathbb{A} : \mathbb{B} = \sum_{ijkl} A_{ijkl} B_{ijkl}$ for any 4-tensors $\mathbb{A} = (A_{ijkl})$ and $\mathbb{B} = (B_{ijkl})$.

The following result holds.

Proposition 3.4. *Let \mathbf{U}_j^α be defined in (3.14), where $j = 1, 2, \dots, n$, for n sufficiently large. Let $J_{\alpha,\beta}$ be defined by (3.24). Then, for all $\mathbf{z}^S \in \Omega$ far from $\partial\Omega$,*

$$(3.25) \quad \frac{1}{n} \sum_{j=1}^n \mathcal{I}_{\text{TD}}[\mathbf{U}_j^P](\mathbf{z}^S) \simeq 4\delta^d \frac{\mu_0}{\omega} \left(\frac{\pi}{\kappa_P} \right)^{d-2} \left(\frac{\kappa_S}{\kappa_P} \right)^2 \left(\frac{1}{c_P} J_{P,P}(\mathbf{z}^S) + \frac{1}{c_S} J_{S,P}(\mathbf{z}^S) \right)$$

and

$$(3.26) \quad \frac{1}{n} \sum_{j=1}^n \mathcal{I}_{\text{TD}}[\mathbf{U}_j^S](\mathbf{z}^S) \simeq 4\delta^d \frac{\mu_0}{\omega} \left(\frac{\pi}{\kappa_S} \right)^{d-2} \left(\frac{1}{c_S} J_{S,S}(\mathbf{z}^S) + \frac{1}{c_P} J_{S,P}(\mathbf{z}^S) \right).$$

Proof. Let us compute \mathcal{I}_{TD} for n P -plane waves, i.e.

$$(3.27) \quad \begin{aligned} \frac{1}{n} \sum_{j=1}^n \mathcal{I}_{\text{TD}}[\mathbf{U}_j^P](\mathbf{z}^S) &= \frac{\delta^d}{\omega} \frac{1}{n} \Re e \sum_{j=1}^n \nabla \mathbf{U}_j^P(\mathbf{z}^S) : \mathbb{M} \left[\mathfrak{S}m \left\{ (\nabla^2 \widetilde{\Gamma}_0^\omega)(\mathbf{z}^S - \mathbf{z}_a) \right\} : \mathbb{M} \overline{\nabla \mathbf{U}_j^P}(\mathbf{z}_a) \right] \\ &\simeq \delta^d \frac{\omega}{c_P^2} \frac{1}{n} \Re e \sum_{j=1}^n e^{i\kappa_P(\mathbf{z}^S - \mathbf{z}_a) \cdot \mathbf{e}_{\theta_j}} \mathbf{e}_{\theta_j} \otimes \mathbf{e}_{\theta_j} \\ &: \mathbb{M} \left(\mathfrak{S}m \left\{ \nabla^2 \widetilde{\Gamma}_0^\omega(\mathbf{z}^S - \mathbf{z}_a) \right\} : \mathbb{M} \mathbf{e}_{\theta_j} \otimes \mathbf{e}_{\theta_j} \right). \end{aligned}$$

Equivalently,

$$(3.28) \quad \begin{aligned} \frac{1}{n} \sum_{j=1}^n \mathcal{I}_{\text{TD}}[\mathbf{U}_j^P](\mathbf{z}^S) &= \delta^d \frac{\omega}{c_P^2} \frac{1}{n} \Re e \sum_{j=1}^n e^{i\kappa_P(\mathbf{z}^S - \mathbf{z}_a) \cdot \mathbf{e}_{\theta_j}} \sum_{i,k,l,m=1}^d \sum_{i',k',l',m'=1}^d A_{ik}^{\theta_j} m_{lmik} \\ &\times \mathfrak{S}m \left\{ \left((\partial_{l'i'}^2 \widetilde{\Gamma}_0^\omega)(\mathbf{z}^S - \mathbf{z}_a) \right)_{mk'} \right\} m_{l'm'i'k'} A_{l'm'}^{\theta_j}, \end{aligned}$$

where the matrix $\mathbf{A}^{\theta_j} = (A_{ik}^{\theta_j})_{ik}$ is defined as $\mathbf{A}^{\theta_j} := \mathbf{e}_{\theta_j} \otimes \mathbf{e}_{\theta_j}$. It follows that

$$(3.29) \quad \begin{aligned} \frac{1}{n} \sum_{j=1}^n \mathcal{I}_{\text{TD}}[\mathbf{U}_j^P](\mathbf{z}^S) &= \delta^d \Re e \sum_{i,k,l,m=1}^d \sum_{i',k',l',m'=1}^d m_{lmik} m_{l'm'i'k'} \mathfrak{S}m \left[\left((\partial_{l'i'}^2 \widetilde{\Gamma}_0^\omega)(\mathbf{z}^S - \mathbf{z}_a) \right)_{mk'} \right] \\ &\times \left(\frac{\omega}{c_P^2} \frac{1}{n} \sum_{j=1}^n e^{i\kappa_P(\mathbf{z}^S - \mathbf{z}_a) \cdot \mathbf{e}_{\theta_j}} A_{ik}^{\theta_j} A_{l'm'}^{\theta_j} \right). \end{aligned}$$

Recall that for n sufficiently large, we have from (3.18)

$$\frac{1}{n} \sum_{j=1}^n e^{i\kappa_P \mathbf{x} \cdot \mathbf{e}_{\theta_j}} \mathbf{e}_{\theta_j} \otimes \mathbf{e}_{\theta_j} \simeq -4\mu_0 \left(\frac{\pi}{\kappa_P}\right)^{d-2} \left(\frac{\kappa_S}{\kappa_P}\right)^2 \Im m \{ \mathbf{\Gamma}_{0,P}^\omega(\mathbf{x}) \}$$

(with the version (3.20) in dimension 3). Taking the Hessian of the previous approximation leads to

$$\begin{aligned} \frac{1}{n} \sum_{j=1}^n e^{i\kappa_P \mathbf{x} \cdot \mathbf{e}_{\theta_j}} \mathbf{e}_{\theta_j} \otimes \mathbf{e}_{\theta_j} \otimes \mathbf{e}_{\theta_j} \otimes \mathbf{e}_{\theta_j} &\simeq 4\mu_0 \frac{c_P^2}{\omega^2} \left(\frac{\pi}{\kappa_P}\right)^{d-2} \left(\frac{\kappa_S}{\kappa_P}\right)^2 \Im m \{ \nabla^2 \mathbf{\Gamma}_{0,P}^\omega(\mathbf{x}) \} \\ (3.30) \qquad \qquad \qquad &\simeq 4\mu_0 \frac{c_P^4}{\omega^2 c_S^2} \left(\frac{\pi}{\kappa_P}\right)^{d-2} \Im m \{ \nabla^2 \mathbf{\Gamma}_{0,P}^\omega(\mathbf{x}) \}. \end{aligned}$$

Then, by virtue of (3.18) and (3.30), we obtain

$$\begin{aligned} \frac{1}{n} \sum_{j=1}^n \mathcal{I}_{\text{TD}}[\mathbf{U}_j^P](\mathbf{z}^S) &\simeq \delta^d \frac{4\mu_0}{\omega} \left(\frac{\pi}{\kappa_P}\right)^{d-2} \left(\frac{\kappa_S}{\kappa_P}\right)^2 \sum_{i,k,l,m=1}^d \sum_{i',k',l',m'=1}^d m_{lmik} m_{l'm'i'k'} \\ &\quad \times \Im m \left\{ \left((\partial_{l'i'}^2 \widetilde{\mathbf{\Gamma}}_0^\omega)(\mathbf{z}^S - \mathbf{z}_a) \right)_{mk'} \right\} \Im m \left\{ \left((\partial_{l'i}^2 \mathbf{\Gamma}_{0,P}^\omega)(\mathbf{z}^S - \mathbf{z}_a) \right)_{m'k} \right\} \\ &\simeq \delta^d \frac{4\mu_0}{\omega} \left(\frac{\pi}{\kappa_P}\right)^{d-2} \left(\frac{\kappa_S}{\kappa_P}\right)^2 \\ &\quad \times \sum_{i,k,i',k'=1}^d \left(\sum_{l,m=1}^d m_{lmik} \Im m \left\{ \left((\partial_{l'i'}^2 \widetilde{\mathbf{\Gamma}}_0^\omega)(\mathbf{z}^S - \mathbf{z}_a) \right)_{mk'} \right\} \right) \\ &\quad \times \left(\sum_{l',m'=1}^d m_{l'm'i'k'} \Im m \left\{ \left((\partial_{l'i}^2 \mathbf{\Gamma}_{0,P}^\omega)(\mathbf{z}^S - \mathbf{z}_a) \right)_{m'k} \right\} \right). \end{aligned}$$

Therefore, by the definition (3.24) of $J_{\alpha,\beta}$, we conclude that

$$\begin{aligned} \frac{1}{n} \sum_{j=1}^n \mathcal{I}_{\text{TD}}[\mathbf{U}_j^P](\mathbf{z}^S) &\simeq \delta^d \frac{4\mu_0}{\omega} \left(\frac{\pi}{\kappa_P}\right)^{d-2} \left(\frac{\kappa_S}{\kappa_P}\right)^2 \left(\mathbb{M} \Im m \left\{ \nabla^2 \widetilde{\mathbf{\Gamma}}_0^\omega(\mathbf{z}^S - \mathbf{z}_a) \right\} \right) \\ &\quad : \left(\mathbb{M} \Im m \left\{ \nabla^2 \mathbf{\Gamma}_{0,P}^\omega(\mathbf{z}^S - \mathbf{z}_a) \right\} \right)^T \\ &\simeq \delta^d \frac{4\mu_0}{\omega} \left(\frac{\pi}{\kappa_P}\right)^{d-2} \left(\frac{\kappa_S}{\kappa_P}\right)^2 \left(\frac{1}{c_P} J_{P,P}(\mathbf{z}^S) + \frac{1}{c_S} J_{S,P}(\mathbf{z}^S) \right). \end{aligned}$$

Similarly, consider the case of S -plane waves and compute \mathcal{I}_{TD} for n directions. We have

$$\begin{aligned}
 \frac{1}{n} \sum_{j=1}^n \mathcal{I}_{\text{TD}}[\mathbf{U}_j^S](\mathbf{z}^S) &= \frac{\delta^d}{\omega} \frac{1}{n} \Re e \sum_{j=1}^n \nabla \mathbf{U}_j^S(\mathbf{z}^S) : \mathbb{M} \left(\Im m \left\{ (\nabla^2 \widetilde{\Gamma}_0^\omega)(\mathbf{z}^S - \mathbf{z}_a) \right\} : \mathbb{M} \overline{\nabla \mathbf{U}_j^S}(\mathbf{z}_a) \right) \\
 &\simeq \delta^d \frac{\omega}{c_S^2} \frac{1}{n} \Re e \sum_{j=1}^n e^{i\kappa_S(\mathbf{z}^S - \mathbf{z}_a) \cdot \mathbf{e}_{\theta_j}} \mathbf{e}_{\theta_j}^\perp \otimes \mathbf{e}_{\theta_j} : \mathbb{M} \\
 &\quad \times \left(\Im m \left\{ (\nabla^2 \widetilde{\Gamma}_0^\omega)(\mathbf{z}^S - \mathbf{z}_a) \right\} : \mathbb{M} \mathbf{e}_{\theta_j}^\perp \otimes \mathbf{e}_{\theta_j} \right) \\
 &\simeq \delta^d \frac{\omega}{c_S^2} \frac{1}{n} \Re e \sum_{j=1}^n e^{i\kappa_S(\mathbf{z}^S - \mathbf{z}_a) \cdot \mathbf{e}_{\theta_j}} \sum_{i,k,l,m=1}^d \sum_{i',k',l',m'=1}^d B_{ik}^{\theta_j} m_{lmik} \\
 (3.31) \quad &\quad \times \Im m \left\{ \left((\partial_{li'}^2 \widetilde{\Gamma}_0^\omega)(\mathbf{z}^S - \mathbf{z}_a) \right)_{mk'} \right\} m_{l'm'i'k'} B_{l'm'}^{\theta_j},
 \end{aligned}$$

where the matrix $\mathbf{B}^{\theta_j} = (B_{ik}^{\theta_j})_{ik}$ is defined as $\mathbf{B}^{\theta_j} = \mathbf{e}_{\theta_j} \otimes \mathbf{e}_{\theta_j}^\perp$. It follows that

$$\begin{aligned}
 \frac{1}{n} \sum_{j=1}^n \mathcal{I}_{\text{TD}}[\mathbf{U}_j^S](\mathbf{z}^S) &= \delta^d \sum_{i,k,l,m=1}^d \sum_{i',k',l',m'=1}^d m_{lmik} m_{l'm'i'k'} \Im m \left[\partial_{li'}^2 \left(\widetilde{\Gamma}_0^\omega(\mathbf{z}^S - \mathbf{z}_a) \right)_{mk'} \right] \\
 (3.32) \quad &\quad \times \left(\frac{\omega}{c_S^2} \frac{1}{n} \sum_{j=1}^n e^{i\kappa_S(\mathbf{z}^S - \mathbf{z}_a) \cdot \mathbf{e}_{\theta_j}} B_{ik}^{\theta_j} B_{l'm'}^{\theta_j} \right).
 \end{aligned}$$

Now, recall from (3.19) that for n sufficiently large, we have

$$\frac{1}{n} \sum_{j=1}^n e^{i\kappa_S \mathbf{x} \cdot \mathbf{e}_{\theta_j}} \mathbf{e}_{\theta_j}^\perp \otimes \mathbf{e}_{\theta_j} \simeq -4\mu_0 \left(\frac{\pi}{\kappa_S} \right)^{d-2} \Im m \left\{ \Gamma_{0,S}^\omega(\mathbf{x}) \right\}.$$

Taking the Hessian of this approximation leads to

$$(3.33) \quad \frac{1}{n} \sum_{j=1}^n e^{i\kappa_S \mathbf{x} \cdot \mathbf{e}_{\theta_j}} \mathbf{e}_{\theta_j} \otimes \mathbf{e}_{\theta_j}^\perp \otimes \mathbf{e}_{\theta_j} \otimes \mathbf{e}_{\theta_j}^\perp \simeq 4\mu_0 \frac{c_S^2}{\omega^2} \left(\frac{\pi}{\kappa_S} \right)^{d-2} \Im m \left\{ \nabla^2 \Gamma_{0,S}^\omega(\mathbf{x}) \right\},$$

where we have made use of the convention

$$(\nabla^2 \Gamma_{0,S}^\omega)_{ijkl} = \partial_{ik} (\Gamma_{0,S}^\omega)_{jl}.$$

Then, by using (3.19), (3.33), and arguments similar to those in the case of P -waves, we arrive at

$$\begin{aligned} \frac{1}{n} \sum_{j=1}^n \mathcal{I}_{\text{TD}}[\mathbf{U}_j^S](\mathbf{z}^S) &\simeq \delta^d \frac{4\mu_0}{\omega} \left(\frac{\pi}{\kappa_S} \right)^{d-2} \sum_{i,k,l,m=1}^d \sum_{i',k',l',m'=1}^d m_{lmik} m_{l'm'ik'} \\ &\quad \times \Im m \left\{ \left((\partial_{i'l'}^2 \widetilde{\Gamma}_0^\omega) \right)_{mk'} (\mathbf{z}^S - \mathbf{z}_a) \right\} \\ &\quad \times \Im m \left\{ \left((\partial_{i'l'}^2 \Gamma_{0,S}^\omega) \right)_{m'k} (\mathbf{z}^S - \mathbf{z}_a) \right\} \\ &\simeq \delta^d \frac{4\mu_0}{\omega} \left(\frac{\pi}{\kappa_S} \right)^{d-2} \left(\mathbb{M} \Im m \left\{ (\nabla^2 \widetilde{\Gamma}_0^\omega) (\mathbf{z}^S - \mathbf{z}_a) \right\} \right) \\ &\quad : \left(\mathbb{M} \Im m \left\{ (\nabla^2 \Gamma_{0,S}^\omega) (\mathbf{z}^S - \mathbf{z}_a) \right\} \right)^T \\ &\simeq \delta^d \frac{4\mu_0}{\omega} \left(\frac{\pi}{\kappa_S} \right)^{d-2} \left(\frac{1}{c_P} J_{P,S}(\mathbf{z}^S) + \frac{1}{c_S} J_{S,S}(\mathbf{z}^S) \right). \end{aligned}$$

This completes the proof. \blacksquare

As observed in section 3.2.1, Proposition 3.4 shows that the resolution of \mathcal{I}_{TD} deteriorates due to the presence of the coupling term

$$(3.34) \quad J_{P,S}(\mathbf{z}^S) = \left(\mathbb{M} \Im m \left\{ (\nabla^2 \Gamma_{0,S}^\omega) (\mathbf{z}^S - \mathbf{z}_a) \right\} \right) : \left(\mathbb{M} \Im m \left\{ (\nabla^2 \Gamma_{0,P}^\omega) (\mathbf{z}^S - \mathbf{z}_a) \right\} \right)^T.$$

3.2.3. Summary. To conclude, we summarize the results of this section below.

- Propositions 3.3 and 3.4 indicate that the imaging function \mathcal{I}_{TD} may not attain its maximum at the true location, \mathbf{z}_a , of the inclusion D .
- In both cases, the resolution of the localization of elastic anomaly D degenerates due to the presence of the coupling terms $\Im m \{ \Gamma_{0,P}^\omega (\mathbf{z}^S - \mathbf{z}_a) \} : \Im m \{ \Gamma_{0,S}^\omega (\mathbf{z}^S - \mathbf{z}_a) \}$ and $J_{P,S}(\mathbf{z}^S)$, respectively.
- In order to enhance imaging resolution to its optimum and ensure that the imaging functional attains its maximum only at the location of the inclusion, one must eradicate the coupling terms.

4. Modified imaging framework. In this section, in order to achieve better localization and resolution properties, we introduce a modified imaging framework based on a weighted Helmholtz decomposition of the TD imaging functional. We will show that the modified framework leads to both a better localization (in the sense that the modified imaging functional attains its maximum at the location of the inclusion) and a better resolution than the classical TD based sensitivity framework. It is worth mentioning that the classical framework performs quite well for the case of the Helmholtz equation [6] and the resolution and localization deteriorations are purely dependent on the elastic nature of the problem, that is, due to the coupling of pressure and shear waves propagating with different wave speeds and polarization directions.

It should be noted that in the case of a density contrast only, the modified imaging functional is still TD based, i.e., obtained as the TD of a discrepancy functional. This holds because of the nonconversion of waves (from shear to compressional and vice versa) in the presence of only a small inclusion with a contrast density, as shown in Lemma 3.2. However, in the presence of a small inclusion with different Lamé coefficients with the background medium, there is a mode conversion through the EMT; see, for instance, [22]. As a consequence, the modified functional proposed here cannot be written in such a case as the topological derivative of a discrepancy functional. It is rather a Kirchhoff-type imaging functional and its resolution and stability analysis differs significantly from the case of a density contrast only.

4.1. Weighted imaging functional. Following [4], we introduce a weighted TD imaging functional \mathcal{I}_W and justify that it provides a better localization of the inclusion D than \mathcal{I}_{TD} . This new functional \mathcal{I}_W can be seen as a correction based on a weighted Helmholtz decomposition of \mathcal{I}_{TD} . In fact, using the standard L^2 -theory of the Helmholtz decomposition (see, for instance, [17]), we find that in the search domain the pressure and the shear components of \mathbf{w} , defined by (3.6), can be written as

$$(4.1) \quad \mathbf{w} = \nabla \times \psi_{\mathbf{w}} + \nabla \phi_{\mathbf{w}}.$$

We define the Helmholtz decomposition operators \mathcal{H}^P and \mathcal{H}^S , respectively, by

$$(4.2) \quad \mathcal{H}^P[\mathbf{w}] := \nabla \phi_{\mathbf{w}} \quad \text{and} \quad \mathcal{H}^S[\mathbf{w}] := \nabla \times \psi_{\mathbf{w}}.$$

Actually, the decomposition $\mathbf{w} = \mathcal{H}^P[\mathbf{w}] + \mathcal{H}^S[\mathbf{w}]$ can be found by solving a Neumann problem in the search domain [17]. Then we multiply the components of \mathbf{w} with c_P and c_S , the background pressure and the shear wave speeds, respectively. Finally, we define \mathcal{I}_W by

$$(4.3) \quad \begin{aligned} \mathcal{I}_W[\mathbf{U}] = c_P \Re e \left\{ -\nabla \mathcal{H}^P[\mathbf{U}] : \mathbb{M}'(B') \nabla \mathcal{H}^P[\mathbf{w}] + \omega^2 \left(\frac{\rho'_1}{\rho_0} - 1 \right) |B'| \mathcal{H}^P[\mathbf{U}] \cdot \mathcal{H}^P[\mathbf{w}] \right\} \\ + c_S \Re e \left\{ -\nabla \mathcal{H}^S[\mathbf{U}] : \mathbb{M}'(B') \nabla \mathcal{H}^S[\mathbf{w}] + \omega^2 \left(\frac{\rho'_1}{\rho_0} - 1 \right) |B'| \mathcal{H}^S[\mathbf{U}] \cdot \mathcal{H}^S[\mathbf{w}] \right\}. \end{aligned}$$

In the next section we rigorously explain why this new functional should be better than imaging functional \mathcal{I}_{TD} .

4.2. Sensitivity analysis of weighted imaging functional. In this section, we explain why imaging functional \mathcal{I}_W attains its maximum at the location \mathbf{z}_a of the true inclusion with a better resolution than \mathcal{I}_{TD} . In fact, as shown in this section, \mathcal{I}_W behaves like the square of the imaginary part of a pressure or a shear Green function depending upon the incident wave. Consequently, it provides a resolution of the order of half a wavelength. For simplicity, we once again consider special cases of only density contrast and only elasticity contrast.

4.2.1. Case I: Density contrast. Suppose $\lambda_0 = \lambda_1$ and $\mu_0 = \mu_1$. Recall that in this case, the wave function \mathbf{w} is given by (3.10). Note that $\mathcal{H}^\alpha[\mathbf{\Gamma}_0^\omega] = \mathbf{\Gamma}_{0,\alpha}^\omega, \alpha \in \{P, S\}$. Therefore, the

imaging functional \mathcal{I}_W at $\mathbf{z}^S \in \Omega$ turns out to be

$$(4.4) \quad \begin{aligned} \mathcal{I}_W[\mathbf{U}](\mathbf{z}^S) = & C\omega^4 \Re \left(c_P \mathcal{H}^P[\mathbf{U}](\mathbf{z}^S) \cdot \left[\left(\int_{\partial\Omega} \overline{\Gamma_0^\omega(\mathbf{x} - \mathbf{z}_a)} \Gamma_{0,P}^\omega(\mathbf{x} - \mathbf{z}^S) d\sigma(\mathbf{x}) \right) \overline{\mathbf{U}}(\mathbf{z}_a) \right] \right. \\ & \left. + c_S \mathcal{H}^S[\mathbf{U}](\mathbf{z}^S) \cdot \left[\left(\int_{\partial\Omega} \overline{\Gamma_0^\omega(\mathbf{x} - \mathbf{z}_a)} \Gamma_{0,S}^\omega(\mathbf{x} - \mathbf{z}^S) d\sigma(\mathbf{x}) \right) \overline{\mathbf{U}}(\mathbf{z}_a) \right] \right). \end{aligned}$$

By using Lemma 3.2, we can easily get

$$(4.5) \quad \begin{aligned} \mathcal{I}_W[\mathbf{U}](\mathbf{z}^S) \simeq & -C\omega^3 \Re \left(\mathcal{H}^P[\mathbf{U}](\mathbf{z}^S) \cdot \left[\Im m \{ \Gamma_{0,P}^\omega(\mathbf{z}^S - \mathbf{z}_a) \} \overline{\mathbf{U}}(\mathbf{z}_a) \right] \right. \\ & \left. + \mathcal{H}^S[\mathbf{U}](\mathbf{z}^S) \cdot \left[\Im m \{ \Gamma_{0,S}^\omega(\mathbf{z}^S - \mathbf{z}_a) \} \overline{\mathbf{U}}(\mathbf{z}_a) \right] \right). \end{aligned}$$

Consider n uniformly distributed directions $(\mathbf{e}_{\theta_1}, \mathbf{e}_{\theta_2}, \dots, \mathbf{e}_{\theta_n})$ on the unit disk or sphere for n sufficiently large. Then, the following proposition holds.

Proposition 4.1. *Let \mathbf{U}_j^α be defined in (3.14), where $j = 1, 2, \dots, n$, for n sufficiently large. Then, for all $\mathbf{z}^S \in \Omega$ far from $\partial\Omega$,*

$$(4.6) \quad \frac{1}{n} \sum_{j=1}^n \mathcal{I}_W[\mathbf{U}_j^P](\mathbf{z}^S) \simeq 4\mu_0 C\omega^3 \left(\frac{\pi}{\kappa_P} \right)^{d-2} \left(\frac{\kappa_S}{\kappa_P} \right)^2 \left| \Im m \{ \Gamma_{0,P}^\omega(\mathbf{z}^S - \mathbf{z}_a) \} \right|^2,$$

and

$$(4.7) \quad \frac{1}{n} \sum_{j=1}^n \mathcal{I}_W[\mathbf{U}_j^S](\mathbf{z}^S) \simeq 4\mu_0 C\omega^3 \left(\frac{\pi}{\kappa_S} \right)^{d-2} \left| \Im m \{ \Gamma_{0,S}^\omega(\mathbf{z}^S - \mathbf{z}_a) \} \right|^2,$$

where C is given by (3.12).

Proof. By using arguments similar to those in Proposition 3.3 and (4.5), we show that the weighted imaging functional \mathcal{I}_W for n P -plane waves is given by

$$\begin{aligned} \frac{1}{n} \sum_{j=1}^n \mathcal{I}_W[\mathbf{U}_j^P](\mathbf{z}^S) &= -C\omega^3 \frac{1}{n} \Re \sum_{j=1}^n \mathbf{U}_j^P(\mathbf{z}^S) \cdot \left[\Im m \{ \Gamma_{0,P}^\omega(\mathbf{z}^S - \mathbf{z}_a) \} \overline{\mathbf{U}_j^P}(\mathbf{z}_a) \right] \\ &\simeq -C\omega^3 \frac{1}{n} \Re \sum_{j=1}^n e^{i\kappa_P(\mathbf{z}^S - \mathbf{z}_a) \cdot \mathbf{e}_{\theta_j}} \mathbf{e}_{\theta_j} \cdot \left[\Im m \{ \Gamma_{0,P}^\omega(\mathbf{z}^S - \mathbf{z}_a) \} \mathbf{e}_{\theta_j} \right] \\ &\simeq 4\mu_0 C\omega^3 \left(\frac{\pi}{\kappa_P} \right)^{d-2} \left(\frac{\kappa_S}{\kappa_P} \right)^2 \left| \Im m \{ \Gamma_{0,P}^\omega(\mathbf{z}^S - \mathbf{z}_a) \} \right|^2. \end{aligned}$$

For n S -plane waves

$$\begin{aligned} \frac{1}{n} \sum_{j=1}^n \mathcal{I}_W[\mathbf{U}_j^S](\mathbf{z}^S) &= -C\omega^3 \frac{1}{n} \sum_{j=1}^n \mathbf{U}_j^S(\mathbf{z}^S) \cdot [\Im m \{ \mathbf{\Gamma}_{0,S}^\omega(\mathbf{z}^S - \mathbf{z}_a) \} \mathbf{U}_j^S(\mathbf{z}_a)] \\ &\simeq -C\omega^3 \frac{1}{n} \sum_{j=1}^n e^{i\kappa_S(\mathbf{z}^S - \mathbf{z}_a) \cdot \mathbf{e}_{\theta_j}} \mathbf{e}_{\theta_j}^\perp \cdot [\Im m \{ \mathbf{\Gamma}_{0,S}^\omega(\mathbf{z}^S - \mathbf{z}_a) \} \mathbf{e}_{\theta_j}^\perp] \\ &\simeq 4\mu_0 C\omega^3 \left(\frac{\pi}{\kappa_S} \right)^{d-2} |\Im m \{ \mathbf{\Gamma}_{0,S}^\omega(\mathbf{z}^S - \mathbf{z}_a) \}|^2, \end{aligned}$$

where one should use the version (3.20) in dimension 3. ■

Proposition 4.1 shows that \mathcal{I}_W attains its maximum at \mathbf{z}_a (see Figure 1), and that the coupling term $\Im m \{ \mathbf{\Gamma}_{0,P}^\omega(\mathbf{z}^S - \mathbf{z}_a) \} : \Im m \{ \mathbf{\Gamma}_{0,S}^\omega(\mathbf{z}^S - \mathbf{z}_a) \}$, responsible for the decreased resolution in \mathcal{I}_{TD} , is absent. Moreover, the resolution using weighted imaging functional \mathcal{I}_W is the Rayleigh one, that is, restricted by the diffraction limit of half a wavelength of the wave impinging upon Ω , thanks to the term $|\Im m \{ \mathbf{\Gamma}_{0,\alpha}^\omega(\mathbf{z}^S - \mathbf{z}_a) \}|^2$. Finally, it is worth mentioning that \mathcal{I}_W is a TD based imaging functional. In fact, it is the TD of the discrepancy functional $c_S \mathcal{E}_f[\mathbf{U}^S] + c_P \mathcal{E}_f[\mathbf{U}^P]$, where \mathbf{U}^S is an S -plane wave and \mathbf{U}^P is a P -plane wave.

4.2.2. Case II: Elasticity contrast. Suppose $\rho_0 = \rho_1$, and assume for simplicity that $\mathbb{M} = \mathbb{M}'(B') = \mathbb{M}(B)$. Then, the weighted imaging functional \mathcal{I}_W reduces to

$$\begin{aligned} \mathcal{I}_W(\mathbf{z}^S) &= -\delta^d \left[c_P \nabla \mathcal{H}^P[\mathbf{U}(\mathbf{z}^S)] : \mathbb{M} \nabla \mathcal{H}^P[\mathbf{w}(\mathbf{z}^S)] + c_S \nabla \mathcal{H}^S[\mathbf{U}(\mathbf{z}^S)] : \mathbb{M} \nabla \mathcal{H}^S \mathbf{w}(\mathbf{z}^S) \right] \\ &= -\delta^d \left[c_P \nabla \mathcal{H}^P[\mathbf{U}(\mathbf{z}^S)] : \mathbb{M} \left(\int_{\partial\Omega} \nabla_{\mathbf{z}_a} \overline{\mathbf{\Gamma}_0^\omega}(\mathbf{x} - \mathbf{z}_a) \nabla_{\mathbf{z}^S} \mathbf{\Gamma}_{0,P}^\omega(\mathbf{x} - \mathbf{z}^S) d\sigma(\mathbf{x}) : \mathbb{M} \overline{\nabla \mathbf{U}}(\mathbf{z}_a) \right) \right. \\ &\quad \left. + c_S \nabla \mathcal{H}^S[\mathbf{U}(\mathbf{z}^S)] : \mathbb{M} \left(\int_{\partial\Omega} \nabla_{\mathbf{z}_a} \overline{\mathbf{\Gamma}_0^\omega}(\mathbf{x} - \mathbf{z}_a) \nabla_{\mathbf{z}^S} \mathbf{\Gamma}_{0,S}^\omega(\mathbf{x} - \mathbf{z}^S) d\sigma(\mathbf{x}) : \mathbb{M} \overline{\nabla \mathbf{U}}(\mathbf{z}_a) \right) \right] \\ &= -\delta^d \left[\nabla \mathcal{H}^P[\mathbf{U}(\mathbf{z}^S)] : \mathbb{M} \left(\Im m \{ (\nabla^2 \mathbf{\Gamma}_{0,P}^\omega)(\mathbf{z}^S - \mathbf{z}_a) \} : \mathbb{M} \overline{\nabla \mathbf{U}}(\mathbf{z}_a) \right) \right. \\ (4.8) \quad &\left. + \nabla \mathcal{H}^S[\mathbf{U}(\mathbf{z}^S)] : \mathbb{M} \left(\Im m \{ (\nabla^2 \mathbf{\Gamma}_{0,S}^\omega)(\mathbf{z}^S - \mathbf{z}_a) \} : \mathbb{M} \overline{\nabla \mathbf{U}}(\mathbf{z}_a) \right) \right]. \end{aligned}$$

We observed in section 3.2.2 that the resolution of \mathcal{I}_{TD} is compromised because of the coupling term $J_{S,P}(\mathbf{z}^S)$. We can cancel out this term by using the weighted imaging functional \mathcal{I}_W . For example, using analogous arguments as in Proposition 3.4, we can easily prove the following result.

Proposition 4.2. *Let \mathbf{U}_j^α be defined in (3.14), where $j = 1, 2, \dots, n$, for n sufficiently large. Let $J_{\alpha,\beta}$ be defined by (3.24). Then, for all $\mathbf{z}^S \in \Omega$ far from $\partial\Omega$,*

$$(4.9) \quad \frac{1}{n} \sum_{j=1}^n \mathcal{I}_W[\mathbf{U}_j^\alpha](\mathbf{z}^S) \simeq 4\delta^d \frac{\mu_0}{\omega} \left(\frac{\pi}{\kappa_\alpha} \right)^{d-2} \left(\frac{\kappa_S}{\kappa_\alpha} \right)^2 J_{\alpha,\alpha}(\mathbf{z}^S), \quad \alpha \in \{P, S\}.$$

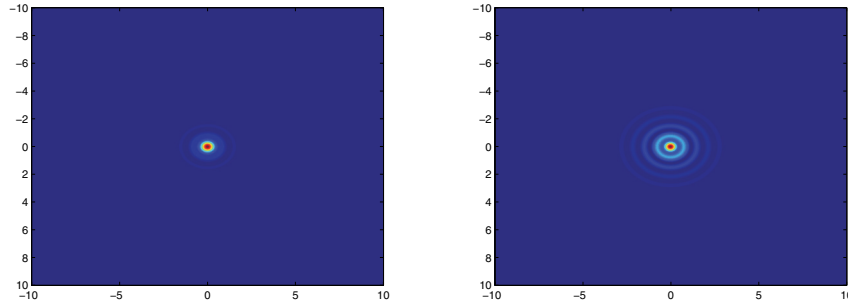


Figure 1. Typical plots of $|\Im\{\Gamma_{0,S}^\omega(\mathbf{z}^S - \mathbf{z}_a)\}|^2$ (on the left) and $|\Im\{\Gamma_{0,P}^\omega(\mathbf{z}^S - \mathbf{z}_a)\}|^2$ (on the right) for $\mathbf{z}_a = \mathbf{0}$ and $c_P/c_S = \sqrt{11}$.

It can be established that \mathcal{I}_W attains its maximum at $\mathbf{z}^S = \mathbf{z}_a$. Consider, for example, the canonical case of a circular or spherical inclusion. The following propositions hold.

Proposition 4.3. *Let D be a disk or a sphere. Then for all search points $\mathbf{z}^S \in \Omega$,*

$$(4.10) \quad J_{P,P}(\mathbf{z}^S) = a^2 \left| \nabla^2 (\Im \Gamma_{0,P}^\omega)(\mathbf{z}^S - \mathbf{z}_a) \right|^2 + 2ab \left| \Delta (\Im \Gamma_{0,P}^\omega)(\mathbf{z}^S - \mathbf{z}_a) \right|^2 + b^2 \left| \Delta \text{Tr}(\Im \Gamma_{0,P}^\omega)(\mathbf{z}^S - \mathbf{z}_a) \right|^2,$$

where Tr represents the trace operator and the constants a and b are defined in (2.19).

Proof. Since

$$(4.11) \quad (\nabla^2 \Gamma_{0,P}^\omega)_{ijkl} = \partial_{ik} (\Gamma_{0,P}^\omega)_{jl},$$

it follows from (2.19) that

$$(4.12) \quad (\mathbb{M} \nabla^2 \Gamma_{0,P}^\omega)_{ijkl} = \sum_{p,q} m_{ijpq} (\nabla^2 \Gamma_{0,P}^\omega)_{pqkl} \\ = \frac{a}{2} \left(\partial_{ik} (\Gamma_{0,P}^\omega)_{jl} + \partial_{jk} (\Gamma_{0,P}^\omega)_{il} \right) + b \sum_{q=1}^d \partial_{qk} (\Gamma_{0,P}^\omega)_{ql} \delta_{ij} \\ (4.13) \quad = \frac{a}{2} \partial_k \left((\nabla \Gamma_{0,P}^\omega \mathbf{e}_l)_{ij} + (\nabla \Gamma_{0,P}^\omega \mathbf{e}_l)_{ij}^T \right) + b \partial_k \nabla \cdot \left((\Gamma_{0,P}^\omega \mathbf{e}_l) \right) \delta_{ij},$$

where \mathbf{e}_l is the unit vector in the direction x_l .

Now, since $\Gamma_{0,P}^\omega \mathbf{e}_l$ is a P -wave, its rotational part vanishes and the gradient is symmetric; i.e.,

$$(4.14) \quad \nabla \times (\Gamma_{0,P}^\omega \mathbf{e}_l) = 0 \quad \text{and} \quad (\nabla \Gamma_{0,P}^\omega \mathbf{e}_l)_{ij} = (\nabla \Gamma_{0,P}^\omega \mathbf{e}_l)_{ji} = (\nabla \Gamma_{0,P}^\omega \mathbf{e}_l)_{ij}^T.$$

Consequently,

$$(4.15) \quad \nabla \nabla \cdot \left((\Gamma_{0,P}^\omega \mathbf{e}_l) \right) = \nabla \times \left(\nabla \times (\Gamma_{0,P}^\omega \mathbf{e}_l) \right) + \Delta \left(\Gamma_{0,P}^\omega \mathbf{e}_l \right) = \Delta \left(\Gamma_{0,P}^\omega \mathbf{e}_l \right),$$

which, together with (4.13) and (4.14), implies

$$(4.16) \quad \mathbb{M} \nabla^2 \Gamma_{0,P}^\omega = a \nabla^2 \Gamma_{0,P}^\omega + b \mathbf{I}_2 \otimes \Delta \Gamma_{0,P}^\omega.$$

Moreover, by the definition of $\Gamma_{0,P}^\omega$, its Hessian, $\nabla^2 \Gamma_{0,P}^\omega$, is also symmetric. Indeed,

$$(4.17) \quad \left(\nabla^2 \Gamma_{0,P}^\omega \right)_{ijkl}^T = \partial_{ki} (\Gamma_{0,P}^\omega)_{lj} = -\frac{\mu_0}{\kappa_S^2} \partial_{kijl} G_P^\omega = \left(\nabla^2 \Gamma_{0,P}^\omega \right)_{ijkl}.$$

Therefore, by virtue of (4.16) and (4.17), $J_{P,P}$ can be rewritten as

$$(4.18) \quad \begin{aligned} J_{P,P}(\mathbf{z}^S) &= \left(a \Im\{(\nabla^2 \Gamma_{0,P}^\omega)(\mathbf{z}^S - \mathbf{z}_a)\} + b \mathbf{I}_2 \otimes \Im\{(\Delta \Gamma_{0,P}^\omega)(\mathbf{z}^S - \mathbf{z}_a)\} \right) \\ &: \left(a \Im\{(\nabla^2 \Gamma_{0,P}^\omega)(\mathbf{z}^S - \mathbf{z}_a)\} + b \Im\{(\Delta \Gamma_{0,P}^\omega)(\mathbf{z}^S - \mathbf{z}_a)\} \otimes \mathbf{I}_2 \right). \end{aligned}$$

Finally, we observe that

$$(4.19) \quad \left(\nabla^2 \Im\{\Gamma_{0,P}^\omega\} \right) : \left(\nabla^2 \Im\{\Gamma_{0,P}^\omega\} \right)^T = \left| \nabla^2 \Im\{\Gamma_{0,P}^\omega\} \right|^2,$$

$$(4.20) \quad \begin{aligned} \nabla^2 \Im\{\Gamma_{0,P}^\omega\} : \left(\mathbf{I}_2 \otimes \Delta \Im\{\Gamma_{0,P}^\omega\} \right) &= \nabla^2 \Im\{\Gamma_{0,P}^\omega\} : \left(\Delta \Im\{\Gamma_{0,P}^\omega\} \otimes \mathbf{I}_2 \right) \\ &= \sum_{i,j,k,l=1}^d \left(\Im(\partial_{ik} \Gamma_{0,P}^\omega)_{jl} \right) \delta_{ij} \Delta \Im(\Gamma_{0,P}^\omega)_{kl} \\ &= \sum_{k,l=1}^d \left(\sum_{i=1}^d \Im(\partial_{ik} \Gamma_{0,P}^\omega)_{il} \right) \Delta \Im(\Gamma_{0,P}^\omega)_{kl} \\ &= \sum_{k,l=1}^d \left(\Delta \Im(\Gamma_{0,P}^\omega)_{kl} \right)^2 \\ &= \left| \Delta \Im\{\Gamma_{0,P}^\omega\} \right|^2, \end{aligned}$$

and

$$(4.21) \quad \begin{aligned} \left(\mathbf{I}_2 \otimes \Delta \Im\{\Gamma_{0,P}^\omega\} \right) : \left(\Delta \Im\{\Gamma_{0,P}^\omega\} \otimes \mathbf{I}_2 \right) &= \sum_{i,j,k,l=1}^d \delta_{ij} \Delta \Im(\Gamma_{0,P}^\omega)_{kl} \delta_{kl} \Delta \Im(\Gamma_{0,P}^\omega)_{ij} \\ &= \sum_{i,k=1}^d \Delta \Im(\Gamma_{0,P}^\omega)_{kk} \Delta \Im(\Gamma_{0,P}^\omega)_{ii} \\ &= \left| \Delta \text{Tr}(\Im\{\Gamma_{0,P}^\omega\}) \right|^2. \end{aligned}$$

We arrive at the conclusion by substituting (4.19), (4.20), and (4.21) in (4.18). ■

Proposition 4.4. *Let D be a disk or a sphere. Then, for all search points $\mathbf{z}^S \in \Omega$,*

$$\begin{aligned}
 J_{S,S}(\mathbf{z}^S) &= \frac{a^2}{\mu_0^2} \left[\frac{1}{\kappa_S^4} \left| \nabla^4 \Im m \{ G_S^\omega(\mathbf{z}^S - \mathbf{z}_a) \} \right|^2 + \frac{(d-6)}{4} \left| \nabla^2 \Im m \{ G_S^\omega(\mathbf{z}^S - \mathbf{z}_a) \} \right|^2 \right. \\
 &\quad \left. + \frac{\kappa_S^4}{4} \left| \Im m \{ G_S^\omega(\mathbf{z}^S - \mathbf{z}_a) \} \right|^2 \right] \\
 &= \frac{a^2}{\mu_0^2} \left[\frac{1}{\kappa_S^4} \sum_{ijkl, k \neq l} \left| \partial_{ijkl} \Im m \{ G_S^\omega(\mathbf{z}^S - \mathbf{z}_a) \} \right|^2 + \frac{(d-2)}{4} \left| \nabla^2 \Im m \{ G_S^\omega(\mathbf{z}^S - \mathbf{z}_a) \} \right|^2 \right. \\
 (4.22) \quad &\quad \left. + \frac{\kappa_S^4}{4} \left| \Im m \{ G_S^\omega(\mathbf{z}^S - \mathbf{z}_a) \} \right|^2 \right],
 \end{aligned}$$

where a is the constant as in (2.19).

Proof. As before, we have

$$\begin{aligned}
 (\mathbb{M} \nabla^2 \Gamma_{0,S}^\omega)_{ijkl} &= \frac{a}{2} \left(\partial_{ik} (\Gamma_{0,S}^\omega)_{jl} + \partial_{jk} (\Gamma_{0,S}^\omega)_{il} \right) + b \partial_k \nabla \cdot \left((\Gamma_{0,S}^\omega e_l) \right) \delta_{ij} \\
 (4.23) \quad &= \frac{a}{2} \left(\partial_{ik} (\Gamma_{0,S}^\omega)_{jl} + \partial_{jk} (\Gamma_{0,S}^\omega)_{il} \right)
 \end{aligned}$$

and

$$(4.24) \quad \left(\mathbb{M} \nabla^2 \Gamma_{0,S}^\omega \right)_{ijkl}^T = \frac{a}{2} \left(\partial_{ik} (\Gamma_{0,S}^\omega)_{jl} + \partial_{il} (\Gamma_{0,S}^\omega)_{jk} \right).$$

Here we have used the facts that $\Gamma_{0,S}^\omega e_l$ is an S -wave, and $\Gamma_{0,S}^\omega$ and its Hessian are symmetric, i.e.,

$$(4.25) \quad \partial_{ik} (\Gamma_{0,S}^\omega)_{jl} = \partial_{ki} (\Gamma_{0,S}^\omega)_{jl} = \partial_{ik} (\Gamma_{0,S}^\omega)_{lj} = \partial_{ki} (\Gamma_{0,S}^\omega)_{lj}.$$

Substituting (4.23) and (4.24) in (3.24), we obtain

$$\begin{aligned}
 J_{S,S}(\mathbf{z}^S) &= \frac{a^2}{4} \sum_{i,j,k,l=1}^d \Im m \left\{ \left((\partial_{ik} \Gamma_{0,S}^\omega)(\mathbf{z}^S - \mathbf{z}_a) \right)_{jl} + \left((\partial_{jk} \Gamma_{0,S}^\omega)(\mathbf{z}^S - \mathbf{z}_a) \right)_{il} \right\} \\
 &\quad \times \Im m \left\{ \left((\partial_{ik} \Gamma_{0,S}^\omega)(\mathbf{z}^S - \mathbf{z}_a) \right)_{jl} + \left((\partial_{il} \Gamma_{0,S}^\omega)(\mathbf{z}^S - \mathbf{z}_a) \right)_{jk} \right\} \\
 (4.26) \quad &:= \frac{a^2}{4} \left(T_1(\mathbf{z}^S) + 2T_2(\mathbf{z}^S) + T_3(\mathbf{z}^S) \right),
 \end{aligned}$$

where

$$\begin{cases} T_1(\mathbf{z}^S) = \sum_{i,j,k,l=1}^d \left(\Im m \left\{ (\partial_{ik} \mathbf{\Gamma}_{0,S}^\omega)_{jl}(\mathbf{z}^S - \mathbf{z}_a) \right\} \right) \left(\Im m \left\{ (\partial_{ik} \mathbf{\Gamma}_{0,S}^\omega)_{jl}(\mathbf{z}^S - \mathbf{z}_a) \right\} \right), \\ T_2(\mathbf{z}^S) = \sum_{i,j,k,l=1}^d \left(\Im m \left\{ (\partial_{ik} \mathbf{\Gamma}_{0,S}^\omega)_{jl}(\mathbf{z}^S - \mathbf{z}_a) \right\} \right) \left(\Im m \left\{ (\partial_{il} \mathbf{\Gamma}_{0,S}^\omega)_{jk}(\mathbf{z}^S - \mathbf{z}_a) \right\} \right), \\ T_3(\mathbf{z}^S) = \sum_{i,j,k,l=1}^d \left(\Im m \left\{ (\partial_{jk} \mathbf{\Gamma}_{0,S}^\omega)_{il}(\mathbf{z}^S - \mathbf{z}_a) \right\} \right) \left(\Im m \left\{ (\partial_{il} \mathbf{\Gamma}_{0,S}^\omega)_{jk}(\mathbf{z}^S - \mathbf{z}_a) \right\} \right). \end{cases}$$

Notice that

$$\Im m \left\{ \mathbf{\Gamma}_{0,S}^\omega(\mathbf{x}) \right\} = \frac{1}{\mu_0 \kappa_S^2} (\kappa_S^2 \mathbf{I}_2 + \mathbb{D}_{\mathbf{x}}) \Im m \left\{ G_S^\omega(\mathbf{x}) \right\},$$

and $\Im m \left\{ G_S^\omega \right\}$ satisfies

$$(4.27) \quad \Delta \Im m \left\{ G_S^\omega \right\}(\mathbf{z}^S - \mathbf{z}_a) + \kappa_S^2 \Im m \left\{ G_S^\omega \right\}(\mathbf{z}^S - \mathbf{z}_a) = 0 \quad \text{for } \mathbf{z}^S \neq \mathbf{z}_a.$$

Therefore, the first term T_1 can be computed as follows:

$$\begin{aligned} T_1(\mathbf{z}^S) &= \left| \nabla^2 (\Im m \mathbf{\Gamma}_{0,S}^\omega)(\mathbf{z}^S - \mathbf{z}_a) \right|^2 \\ &= \frac{1}{\mu_0^2 \kappa_S^4} \sum_{i,j,k,l=1}^d \left[\left(\partial_{ijkl} (\Im m G_S^\omega)(\mathbf{z}^S - \mathbf{z}_a) \right)^2 + \kappa_S^4 \delta_{jl} \left(\partial_{ik} (\Im m G_S^\omega)(\mathbf{z}^S - \mathbf{z}_a) \right)^2 \right. \\ &\quad \left. + 2 \kappa_S^2 \delta_{jl} \partial_{ik} (\Im m G_S^\omega)(\mathbf{z}^S - \mathbf{z}_a) \partial_{ijkl} (\Im m G_S^\omega)(\mathbf{z}^S - \mathbf{z}_a) \right]. \end{aligned}$$

We also have

$$\begin{aligned} &\sum_{i,j,k,l=1}^d 2 \delta_{jl} \partial_{ik} (\Im m G_S^\omega)(\mathbf{z}^S - \mathbf{z}_a) \left(\partial_{ijkl} (\Im m G_S^\omega)(\mathbf{z}^S - \mathbf{z}_a) \right) \\ &= 2 \sum_{i,k=1}^d \left(\partial_{ik} (\Im m G_S^\omega)(\mathbf{z}^S - \mathbf{z}_a) \right) \left(\partial_{ik} \sum_{l=1}^d \partial_{ll} (\Im m G_S^\omega)(\mathbf{z}^S - \mathbf{z}_a) \right) \\ &= -2 \kappa_S^2 \sum_{i,k=1}^d \left(\partial_{ik} (\Im m G_S^\omega)(\mathbf{z}^S - \mathbf{z}_a) \right)^2 \end{aligned}$$

and

$$\sum_{i,j,k,l=1}^d \delta_{jl} \left(\partial_{ik} (\Im m G_S^\omega)(\mathbf{z}^S - \mathbf{z}_a) \right)^2 = d \sum_{i,k=1}^d \left(\partial_{ik} (\Im m G_S^\omega)(\mathbf{z}^S - \mathbf{z}_a) \right)^2.$$

Consequently, we have

$$(4.28) \quad \begin{aligned} T_1(\mathbf{z}^S) &= \left| \nabla^2(\Im m \Gamma_{0,S}^\omega)(\mathbf{z}^S - \mathbf{z}_a) \right|^2 = \frac{1}{\mu_0^2 \kappa_S^4} \left| \nabla^4(\Im m G_S^\omega)(\mathbf{z}^S - \mathbf{z}_a) \right|^2 \\ &\quad + \frac{(d-2)}{\mu_0^2} \sum_{i,k=1}^d \left(\partial_{ik}(\Im m G_S^\omega)(\mathbf{z}^S - \mathbf{z}_a) \right)^2. \end{aligned}$$

Estimation of the term T_2 is quite similar. Indeed,

$$\begin{aligned} T_2(\mathbf{z}^S) &= \frac{1}{\mu_0^2 \kappa_S^4} \sum_{i,j,k,l=1}^d \left[\left(\partial_{ijkl}(\Im m G_S^\omega)(\mathbf{z}^S - \mathbf{z}_a) \right)^2 \right. \\ &\quad \left. + 2\kappa_S^2 \delta_{jl} \partial_{ik}(\Im m G_S^\omega)(\mathbf{z}^S - \mathbf{z}_a) \partial_{ijkl}(\Im m G_S^\omega)(\mathbf{z}^S - \mathbf{z}_a) \right. \\ &\quad \left. + \kappa_S^4 \delta_{jl} \delta_{jk} \left(\partial_{ik}(\Im m G_S^\omega)(\mathbf{z}^S - \mathbf{z}_a) \right) \left(\partial_{il}(\Im m G_S^\omega)(\mathbf{z}^S - \mathbf{z}_a) \right) \right]. \end{aligned}$$

Finally, using

$$\sum_{i,j,k,l=1}^d \delta_{jl} \delta_{jk} \left(\partial_{ik}(\Im m G_S^\omega)(\mathbf{z}^S - \mathbf{z}_a) \right) \left(\partial_{il}(\Im m G_S^\omega)(\mathbf{z}^S - \mathbf{z}_a) \right) = \sum_{i,k=1}^d \left(\partial_{ik}(\Im m G_S^\omega)(\mathbf{z}^S - \mathbf{z}_a) \right)^2,$$

we obtain that

$$(4.29) \quad T_2(\mathbf{z}^S) = \frac{1}{\mu_0^2 \kappa_S^4} \left| \nabla^4(\Im m G_S^\omega)(\mathbf{z}^S - \mathbf{z}_a) \right|^2 - \frac{1}{\mu_0^2} \left| \nabla^2(\Im m G_S^\omega)(\mathbf{z}^S - \mathbf{z}_a) \right|^2.$$

Similarly,

$$\begin{aligned} T_3(\mathbf{z}^S) &= \frac{1}{\mu_0^2 \kappa_S^4} \sum_{i,j,k,l=1}^d \left[\left(\partial_{ijkl}(\Im m G_S^\omega)(\mathbf{z}^S - \mathbf{z}_a) \right)^2 \right. \\ &\quad \left. + 2\kappa_S^2 \delta_{jl} \partial_{ik}(\Im m G_S^\omega)(\mathbf{z}^S - \mathbf{z}_a) \left(\partial_{ijkl}(\Im m G_S^\omega)(\mathbf{z}^S - \mathbf{z}_a) \right) \right. \\ &\quad \left. + \kappa_S^4 \delta_{il} \delta_{jk} \left(\partial_{jk}(\Im m G_S^\omega)(\mathbf{z}^S - \mathbf{z}_a) \right) \left(\partial_{il}(\Im m G_S^\omega)(\mathbf{z}^S - \mathbf{z}_a) \right) \right]. \end{aligned}$$

By virtue of

$$\begin{aligned} &\sum_{i,j,k,l=1}^d \delta_{il} \delta_{jk} \left(\partial_{jk}(\Im m G_S^\omega)(\mathbf{z}^S - \mathbf{z}_a) \right) \left(\partial_{il}(\Im m G_S^\omega)(\mathbf{z}^S - \mathbf{z}_a) \right) \\ &= \sum_{i,k=1}^d \left(\partial_{kk}(\Im m G_S^\omega)(\mathbf{z}^S - \mathbf{z}_a) \right) \left(\partial_{ii}(\Im m G_S^\omega)(\mathbf{z}^S - \mathbf{z}_a) \right) \\ &= \kappa_S^4 \left(\Im m G_S^\omega(\mathbf{z}^S - \mathbf{z}_a) \right)^2, \end{aligned}$$

we have

$$\begin{aligned}
 T_3(\mathbf{z}^S) &= \frac{1}{\mu_0^2 \kappa_S^4} \left| \nabla^4 (\Im m G_S^\omega)(\mathbf{z}^S - \mathbf{z}_a) \right|^2 - \frac{2}{\mu_0^2} \left| \nabla^2 (\Im m G_S^\omega)(\mathbf{z}^S - \mathbf{z}_a) \right|^2 \\
 (4.30) \quad &+ \frac{\kappa_S^4}{\mu_0^2} \left| \Im m G_S^\omega(\mathbf{z}^S - \mathbf{z}_a) \right|^2.
 \end{aligned}$$

We conclude the proof by substituting (4.28), (4.29), and (4.30) in (4.26) and using again (4.27). ■

Figure 2 shows typical plots of $J_{\alpha,\alpha}$ for $\alpha \in \{P, S\}$.

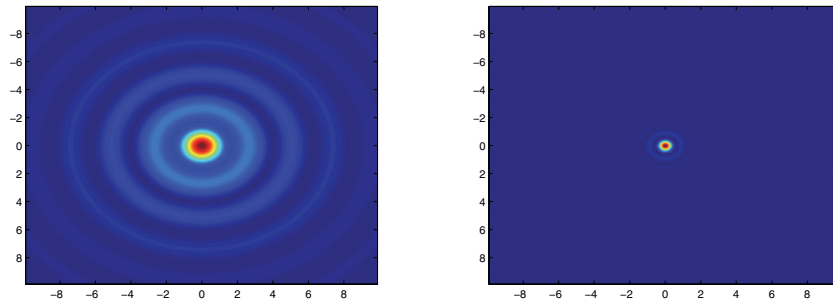


Figure 2. Typical plots of $J_{P,P}$ (on the left) and $J_{S,S}$ (on the right) for $\mathbf{z}_a = \mathbf{0}$ and $c_P/c_S = \sqrt{11}$.

5. Statistical stability with measurement noise. Let \mathbf{U}_j^P and \mathbf{U}_j^S be as before. Let $\{\mathbf{U}_j\}$ be plane waves. Define

$$(5.1) \quad \mathcal{I}_{\text{WF}}[\{\mathbf{U}_j\}](\mathbf{z}^S) = \frac{1}{n} \sum_{j=1}^n \mathcal{I}_{\text{W}}[\mathbf{U}_j](\mathbf{z}^S).$$

In the previous section, we have analyzed the resolution of the imaging functional \mathcal{I}_{WF} in the ideal situation where the measurement \mathbf{u}_{meas} is accurate. Here, we analyze how the result will be modified when the measurement is corrupted by noise.

5.1. Measurement noise model. We consider the simplest model for the measurement noise. Let \mathbf{u}_{true} be the accurate value of the elastic displacement field. The measurement \mathbf{u}_{meas} is then

$$(5.2) \quad \mathbf{u}_{\text{meas}}(\mathbf{x}) = \mathbf{u}_{\text{true}}(\mathbf{x}) + \boldsymbol{\nu}_{\text{noise}}(\mathbf{x}),$$

which is the accurate value corrupted by measurement noise modeled as $\boldsymbol{\nu}_{\text{noise}}(\mathbf{x})$, $\mathbf{x} \in \partial\Omega$. Note that $\boldsymbol{\nu}_{\text{noise}}(\mathbf{x})$ is valued in \mathbb{C}^d , $d = 2, 3$.

Let \mathbb{E} denote the expectation with respect to the statistics of the measurement noise. We assume that $\{\boldsymbol{\nu}_{\text{noise}}(\mathbf{x}), \mathbf{x} \in \partial\Omega\}$ is mean-zero circular Gaussian and satisfies

$$(5.3) \quad \mathbb{E}[\boldsymbol{\nu}_{\text{noise}}(\mathbf{y}) \otimes \overline{\boldsymbol{\nu}_{\text{noise}}(\mathbf{y}')}^T] = \sigma_{\text{noise}}^2 \delta_{\mathbf{y}}(\mathbf{y}') \mathbf{I}_2.$$

This means that first, the measurement noises at different locations on the boundary are uncorrelated; second, different components of the measurement noise are uncorrelated; and third, the real and imaginary parts are uncorrelated. Finally, the noise has variance σ_{noise}^2 .

In the imaging functional \mathcal{I}_{WF} , the elastic medium is probed by multiple plane waves with different propagating directions, and consequently multiple measurements are obtained at the boundary accordingly. We assume that two measurements corresponding to two different plane wave propagations are uncorrelated. Therefore, it holds that

$$(5.4) \quad \mathbb{E}[\boldsymbol{\nu}_{\text{noise}}^j(\mathbf{y}) \otimes \overline{\boldsymbol{\nu}_{\text{noise}}^l(\mathbf{y}')}] = \sigma_{\text{noise}}^2 \delta_{jl} \delta_{\mathbf{y}}(\mathbf{y}') \mathbf{I}_2,$$

where j and l are labels for the measurements and δ_{jl} is the Kronecker symbol.

5.2. Propagation of measurement noise in the backpropagation step. The measurement noise affects the TD based imaging functional through the backpropagation step which builds the function \mathbf{w} in (3.6). Due to the noise, we have

$$(5.5) \quad \mathbf{w}(\mathbf{x}) = \mathcal{S}_{\Omega}^{\omega} \left[\overline{\left(\frac{1}{2}I - \mathcal{K}_{\Omega}^{\omega} \right) [\mathbf{U} - \mathbf{u}_{\text{true}} - \boldsymbol{\nu}_{\text{noise}}]} \right] (\mathbf{x}) = \mathbf{w}_{\text{true}}(\mathbf{x}) + \mathbf{w}_{\text{noise}}(\mathbf{x})$$

for $\mathbf{x} \in \Omega$. Here, \mathbf{w}_{true} is the result of backpropagating only the accurate data, while $\mathbf{w}_{\text{noise}}$ is that of backpropagating the measurement noise. In particular,

$$(5.6) \quad \mathbf{w}_{\text{noise}}(\mathbf{x}) = -\mathcal{S}_{\Omega}^{\omega} \left[\overline{\left(\frac{1}{2}I - \mathcal{K}_{\Omega}^{\omega} \right) [\boldsymbol{\nu}_{\text{noise}}]} \right] (\mathbf{x}), \quad \mathbf{x} \in \Omega.$$

To analyze the statistics of $\mathbf{w}_{\text{noise}}$, we proceed in two steps. First define

$$(5.7) \quad \boldsymbol{\nu}_{\text{noise},1}(\mathbf{x}) = \left(\frac{1}{2}I - \mathcal{K}_{\Omega}^{\omega} \right) [\boldsymbol{\nu}_{\text{noise}}](\mathbf{x}), \quad \mathbf{x} \in \partial\Omega.$$

Then, due to linearity, $\boldsymbol{\nu}_{\text{noise},1}$ is also a mean-zero circular Gaussian random process. Its covariance function can be calculated as

$$\begin{aligned} \mathbb{E}[\boldsymbol{\nu}_{\text{noise},1}(\mathbf{y}) \otimes \overline{\boldsymbol{\nu}_{\text{noise},1}(\mathbf{y}')}] &= \frac{1}{4} \mathbb{E}[\boldsymbol{\nu}_{\text{noise}}(\mathbf{y}) \otimes \overline{\boldsymbol{\nu}_{\text{noise}}(\mathbf{y}')}] - \frac{1}{2} \mathbb{E}[\mathcal{K}_{\Omega}^{\omega}[\boldsymbol{\nu}_{\text{noise}}](\mathbf{y}) \otimes \overline{\boldsymbol{\nu}_{\text{noise}}(\mathbf{y}')}] \\ &\quad - \frac{1}{2} \mathbb{E}[\boldsymbol{\nu}_{\text{noise}}(\mathbf{y}) \otimes \overline{\mathcal{K}_{\Omega}^{\omega}[\boldsymbol{\nu}_{\text{noise}}](\mathbf{y}')}] + \mathbb{E}[\mathcal{K}_{\Omega}^{\omega}[\boldsymbol{\nu}_{\text{noise}}](\mathbf{y}) \otimes \overline{\mathcal{K}_{\Omega}^{\omega}[\boldsymbol{\nu}_{\text{noise}}](\mathbf{y}')}]. \end{aligned}$$

The terms on the right-hand side can be evaluated using the statistics of $\boldsymbol{\nu}_{\text{noise}}$ and the explicit expression of $\mathcal{K}_{\Omega}^{\omega}$. Let us calculate the last term. It has the expression

$$\mathbb{E} \left[\int_{\partial\Omega} \int_{\partial\Omega} \left[\frac{\partial \Gamma_0^{\omega}}{\partial \nu_{\mathbf{x}}}(\mathbf{y} - \mathbf{x}) \boldsymbol{\nu}_{\text{noise}}(\mathbf{x}) \right] \otimes \overline{\left[\frac{\partial \Gamma_0^{\omega}}{\partial \nu_{\mathbf{x}'}}(\mathbf{y}' - \mathbf{x}') \boldsymbol{\nu}_{\text{noise}}(\mathbf{x}') \right]} d\sigma(\mathbf{x}) d\sigma(\mathbf{x}') \right].$$

Using the coordinate representations and the summation convention, we can calculate the jk th element of this matrix by

$$\begin{aligned} &\int_{\partial\Omega} \int_{\partial\Omega} \left[\frac{\partial \Gamma_0^{\omega}}{\partial \nu_{\mathbf{x}}}(\mathbf{y} - \mathbf{x}) \right]_{jl} \left[\frac{\partial \overline{\Gamma_0^{\omega}}}{\partial \nu_{\mathbf{x}'}}(\mathbf{y}' - \mathbf{x}') \right]_{ks} \mathbb{E}[\boldsymbol{\nu}_{\text{noise}}(\mathbf{x}) \otimes \overline{\boldsymbol{\nu}_{\text{noise}}(\mathbf{x}')}]_{ls} d\sigma(\mathbf{x}) d\sigma(\mathbf{x}') \\ &= \sigma_{\text{noise}}^2 \int_{\partial\Omega} \left[\frac{\partial \Gamma_0^{\omega}}{\partial \nu_{\mathbf{x}}}(\mathbf{y} - \mathbf{x}) \right]_{js} \left[\frac{\partial \overline{\Gamma_0^{\omega}}}{\partial \nu_{\mathbf{x}'}}(\mathbf{y}' - \mathbf{x}) \right]_{ks} d\sigma(\mathbf{x}) \\ &= \sigma_{\text{noise}}^2 \int_{\partial\Omega} \frac{\partial \Gamma_0^{\omega}}{\partial \nu_{\mathbf{x}}}(\mathbf{y} - \mathbf{x}) \frac{\partial \overline{\Gamma_0^{\omega}}}{\partial \nu_{\mathbf{x}}}(\mathbf{x} - \mathbf{y}') d\sigma(\mathbf{x}). \end{aligned}$$

In the last step, we used the reciprocity relation

$$(5.8) \quad \Gamma_0^\omega(\mathbf{y} - \mathbf{x}) = [\Gamma_0^\omega(\mathbf{x} - \mathbf{y})]^T$$

for any $\mathbf{x}, \mathbf{y} \in \mathbb{R}^d$.

The other terms in the covariance function of $\boldsymbol{\nu}_{\text{noise},1}$ can be similarly calculated. Consequently, we have

$$(5.9) \quad \begin{aligned} \mathbb{E}[\boldsymbol{\nu}_{\text{noise},1}(\mathbf{y}) \otimes \overline{\boldsymbol{\nu}_{\text{noise},1}(\mathbf{y}')}] &= \frac{\sigma_{\text{noise}}^2}{4} \delta_{\mathbf{y}}(\mathbf{y}') \mathbf{I}_2 - \frac{\sigma_{\text{noise}}^2}{2} \left[\frac{\partial \Gamma_0^\omega}{\partial \nu_{\mathbf{y}'}}(\mathbf{y} - \mathbf{y}') + \frac{\partial \overline{\Gamma_0^\omega}}{\partial \nu_{\mathbf{y}}}(\mathbf{y} - \mathbf{y}') \right] \\ &+ \sigma_{\text{noise}}^2 \int_{\partial\Omega} \frac{\partial \Gamma_0^\omega}{\partial \nu_{\mathbf{x}}}(\mathbf{y} - \mathbf{x}) \frac{\partial \overline{\Gamma_0^\omega}}{\partial \nu_{\mathbf{x}}}(\mathbf{x} - \mathbf{y}') d\sigma(\mathbf{x}). \end{aligned}$$

From the expression of \mathcal{I}_{WF} and \mathcal{I}_{W} , we see that only the Helmholtz decomposition of \mathbf{w}_{meas} , that is, $\mathcal{H}^P[\mathbf{w}]$ and $\mathcal{H}^S[\mathbf{w}]$, is used in the imaging functional. Define $\mathbf{w}^\alpha = \mathcal{H}^\alpha[\mathbf{w}]$, $\alpha \in \{P, S\}$. Using the decomposition in (5.5), we can similarly define $\mathbf{w}_{\text{true}}^\alpha$ and $\mathbf{w}_{\text{noise}}^\alpha$. In particular, we find that

$$\mathbf{w}_{\text{noise}}^\alpha(\mathbf{x}) = - \int_{\partial\Omega} \Gamma_{0,\alpha}^\omega(\mathbf{x} - \mathbf{y}) \overline{\boldsymbol{\nu}_{\text{noise},1}(\mathbf{y})} d\sigma(\mathbf{y}), \quad \mathbf{x} \in \Omega.$$

This is a mean-zero \mathbb{C}^d -valued circular Gaussian random field with parameters in Ω . The jk th element of its covariance function is evaluated by

$$\mathbb{E}[\mathbf{w}_{\text{noise}}^\alpha(\mathbf{x}) \otimes \overline{\mathbf{w}_{\text{noise}}^\alpha(\mathbf{x}')}]_{jk} = \sum_{l,s} \int_{(\partial\Omega)^2} (\Gamma_{0,\alpha}^\omega(\mathbf{x} - \mathbf{y}))_{jl} (\overline{\Gamma_{0,\alpha}^\omega(\mathbf{x}' - \mathbf{y}')})_{ks} \mathbb{E}[\overline{\boldsymbol{\nu}_{\text{noise},1}(\mathbf{y})} \otimes \boldsymbol{\nu}_{\text{noise},1}(\mathbf{y}')]_{ls}.$$

Using the statistics of $\boldsymbol{\nu}_{\text{noise},1}$ derived above, we find that

$$\begin{aligned} \mathbb{E}[\mathbf{w}_{\text{noise}}^\alpha(\mathbf{x}) \otimes \overline{\mathbf{w}_{\text{noise}}^\alpha(\mathbf{x}')}] &= \frac{\sigma_{\text{noise}}^2}{4} \int_{\partial\Omega} \Gamma_{0,\alpha}^\omega(\mathbf{x} - \mathbf{y}) \overline{\Gamma_{0,\alpha}^\omega(\mathbf{y} - \mathbf{x}')} d\sigma(\mathbf{y}) \\ &- \frac{\sigma_{\text{noise}}^2}{2} \int_{(\partial\Omega)^2} \Gamma_{0,\alpha}^\omega(\mathbf{x} - \mathbf{y}) \left[\frac{\partial \Gamma_0^\omega}{\partial \nu_{\mathbf{y}}}(\mathbf{y} - \mathbf{y}') + \frac{\partial \overline{\Gamma_0^\omega}}{\partial \nu_{\mathbf{y}'}}(\mathbf{y} - \mathbf{y}') \right] \overline{\Gamma_{0,\alpha}^\omega(\mathbf{y}' - \mathbf{x}')} d\sigma(\mathbf{y}) d\sigma(\mathbf{y}') \\ &+ \sigma_{\text{noise}}^2 \int_{(\partial\Omega)^3} \Gamma_{0,\alpha}^\omega(\mathbf{x} - \mathbf{y}) \frac{\partial \overline{\Gamma_0^\omega}}{\partial \nu_{\mathbf{z}}}(\mathbf{y} - \mathbf{z}) \frac{\partial \Gamma_0^\omega}{\partial \nu_{\mathbf{z}}}(\mathbf{z} - \mathbf{y}') \overline{\Gamma_{0,\alpha}^\omega(\mathbf{y}' - \mathbf{x}')} d\sigma(\mathbf{z}) d\sigma(\mathbf{y}) d\sigma(\mathbf{y}'). \end{aligned}$$

Thanks to the Helmholtz–Kirchhoff identities, the above expression is simplified to

$$\begin{aligned} \mathbb{E}[\mathbf{w}_{\text{noise}}^\alpha(\mathbf{x}) \otimes \overline{\mathbf{w}_{\text{noise}}^\alpha(\mathbf{x}')}] &= - \frac{\sigma_{\text{noise}}^2}{4c_\alpha\omega} \Im m\{\Gamma_{0,\alpha}^\omega(\mathbf{x} - \mathbf{x}')\} \\ &+ \frac{\sigma_{\text{noise}}^2}{2c_\alpha\omega} \int_{\partial\Omega} \Gamma_{0,\alpha}^\omega(\mathbf{x} - \mathbf{y}) \frac{\partial \Im m\{\Gamma_{0,\alpha}^\omega(\mathbf{y} - \mathbf{x}')\}}{\partial \nu_{\mathbf{y}}} d\sigma(\mathbf{y}) \\ &+ \frac{\sigma_{\text{noise}}^2}{2c_\alpha\omega} \int_{\partial\Omega} \frac{\partial \Im m\{\Gamma_{0,\alpha}^\omega(\mathbf{x} - \mathbf{y}')\}}{\partial \nu_{\mathbf{y}'}} \overline{\Gamma_{0,\alpha}^\omega(\mathbf{y}' - \mathbf{x}')} d\sigma(\mathbf{y}') \\ &- \frac{\sigma_{\text{noise}}^2}{(c_\alpha\omega)^2} \int_{\partial\Omega} \frac{\partial \Im m\{\Gamma_{0,\alpha}^\omega(\mathbf{x} - \mathbf{z})\}}{\partial \nu_{\mathbf{z}}} \frac{\partial \Im m\{\Gamma_{0,\alpha}^\omega(\mathbf{z} - \mathbf{x}')\}}{\partial \nu_{\mathbf{z}}} d\sigma(\mathbf{z}). \end{aligned}$$

Assuming that \mathbf{x}, \mathbf{x}' are far away from the boundary, we have from [4] the asymptotic formula

$$(5.10) \quad \frac{\partial \Gamma_{0,\alpha}^\omega(\mathbf{x} - \mathbf{y})}{\partial \nu_{\mathbf{y}}} \simeq i c_\alpha \omega \Gamma_{0,\alpha}^\omega(\mathbf{x} - \mathbf{y}),$$

where the error is of order $o(|\mathbf{x} - \mathbf{y}|^{1/2-d})$. Using this asymptotic formula and the Helmholtz–Kirchhoff identity (taking the imaginary part of the identity), we obtain

$$(5.11) \quad \mathbb{E}[\mathbf{w}_{\text{noise}}^\alpha(\mathbf{x}) \otimes \overline{\mathbf{w}_{\text{noise}}^\alpha(\mathbf{x}')}] = -\frac{\sigma_{\text{noise}}^2}{4c_\alpha \omega} \Im m\{\Gamma_{0,\alpha}^\omega(\mathbf{x} - \mathbf{x}')\}.$$

In conclusion, the random field $\mathbf{w}_{\text{noise}}^\alpha(\mathbf{x})$, $\mathbf{x} \in \Omega$, is a Gaussian field with mean zero and covariance function (5.11). It is a speckle pattern, i.e., a random cloud of hot spots where typical diameters are of the order of the wavelength and whose typical amplitudes are of the order of $\sigma_{\text{noise}}/(2\sqrt{c_\alpha \omega})$.

5.3. Stability analysis. Now we are ready to analyze the statistical stability of the imaging functional \mathcal{I}_{WF} . As before, we consider separate cases where the medium has only density contrast or only elastic contrast.

5.3.1. Case I: Density contrast. Using the facts that the plane waves \mathbf{U}^P are irrotational and that the plane waves \mathbf{U}^S are solenoidal, we see that for a searching point $\mathbf{z} \in \Omega$ and for $\alpha \in \{P, S\}$,

$$\mathcal{I}_{\text{WF}}[\{\mathbf{U}_j^\alpha\}](\mathbf{z}) = c_\alpha \omega^2 \left(\frac{\rho'_1}{\rho_0} - 1 \right) |B'| \frac{1}{n} \sum_{j=1}^n \Re e\{\mathbf{U}_j^\alpha(\mathbf{z}) \cdot (\mathbf{w}_{j,\text{true}}^\alpha(\mathbf{z}) + \mathbf{w}_{j,\text{noise}}^\alpha(\mathbf{z}))\}.$$

We observe the following: The contribution of $\{\mathbf{w}_{j,\text{true}}^\alpha\}$ is exactly that in Proposition 4.1. On the other hand, the contribution of $\{\mathbf{w}_{j,\text{noise}}^\alpha\}$ forms a field corrupting the true image. With $C_\alpha := c_\alpha \omega^2 |B'| (\rho'_1/\rho_0 - 1)$, the covariance function of the corrupted image can be calculated as follows. Let $\mathbf{z}' \in \Omega$. We have

$$\begin{aligned} \text{Cov}(\mathcal{I}_{\text{WF}}[\{\mathbf{U}_j^\alpha\}](\mathbf{z}), \mathcal{I}_{\text{WF}}[\{\mathbf{U}_j^\alpha\}](\mathbf{z}')) &= C_\alpha^2 \frac{1}{n^2} \sum_{j,l=1}^n \mathbb{E}[\Re e\{\mathbf{U}_j^\alpha \cdot \mathbf{w}_{j,\text{noise}}^\alpha\} \Re e\{\mathbf{U}_l^\alpha \cdot \mathbf{w}_{l,\text{noise}}^\alpha\}] \\ &= C_\alpha^2 \frac{1}{2n^2} \sum_{j=1}^n \Re e\left\{ \mathbf{U}_j^\alpha(\mathbf{z}) \cdot \mathbb{E}[\mathbf{w}_{j,\text{noise}}^\alpha(\mathbf{z}) \otimes \overline{\mathbf{w}_{j,\text{noise}}^\alpha(\mathbf{z}')}] \overline{\mathbf{U}_j^\alpha(\mathbf{z}')} \right\}. \end{aligned}$$

To get the second equality, we used the fact that $\mathbf{w}_{j,\text{noise}}^\alpha$ and $\mathbf{w}_{l,\text{noise}}^\alpha$ are uncorrelated unless $j = l$. Thanks to the statistics (5.11), the covariance of the image is given by

$$-C_\alpha^2 \frac{\sigma_{\text{noise}}^2}{4c_\alpha \omega} \frac{1}{2n^2} \Re e \sum_{j=1}^n e^{i\kappa_\alpha(\mathbf{z}-\mathbf{z}') \cdot \mathbf{e}_{\theta_j}} \mathbf{e}_{\theta_j}^\alpha \cdot [\Im m\{\Gamma_{0,\alpha}^\omega(\mathbf{z} - \mathbf{z}')\}] \mathbf{e}_{\theta_j}^\alpha,$$

where $\mathbf{e}_{\theta_j}^P = \mathbf{e}_{\theta_j}$ and $\mathbf{e}_{\theta_j}^S = \mathbf{e}_{\theta_j}^\perp$.

Using the same arguments as those in the proof of Proposition 4.1, we obtain that

$$(5.12) \quad \text{Cov}(\mathcal{I}_{\text{WF}}[\{\mathbf{U}_j^\alpha\}](\mathbf{z}), \mathcal{I}_{\text{WF}}[\{\mathbf{U}_j^\alpha\}](\mathbf{z}')) = C'_\alpha \frac{\sigma_{\text{noise}}^2}{2n} |\Im\{\mathbf{\Gamma}_{0,\alpha}^\omega(\mathbf{z} - \mathbf{z}')\}|^2,$$

where the constant

$$C'_\alpha = c_\alpha \omega^3 \mu_0 |B'|^2 \left(\frac{\rho'_1}{\rho_0} - 1\right)^2 \left(\frac{\pi}{\kappa_\alpha}\right)^{d-2} \left(\frac{\kappa_S}{\kappa_\alpha}\right)^2.$$

The following remarks hold. First, the perturbation due to noise has small typical values of order $\sigma_{\text{noise}}/\sqrt{2n}$ and slightly affects the peak of the imaging functional \mathcal{I}_{WF} . Second, the typical shape of the hot spot in the perturbation due to the noise is exactly of the form of the main peak of \mathcal{I}_{WF} obtained in the absence of noise. Third, the use of multiple directional plane waves reduces the effect of measurement noise on the image quality.

From (5.12) it follows that the variance of the imaging functional \mathcal{I}_{WF} at the search point \mathbf{z} is given by

$$(5.13) \quad \text{Var}(\mathcal{I}_{\text{WF}}[\{\mathbf{U}_j^\alpha\}](\mathbf{z})) = C'_\alpha \frac{\sigma_{\text{noise}}^2}{2n} |\Im\{\mathbf{\Gamma}_{0,\alpha}^\omega(\mathbf{0})\}|^2.$$

Define the signal-to-noise ratio (SNR) by

$$\text{SNR} := \frac{\mathbb{E}[\mathcal{I}_{\text{WF}}[\{\mathbf{U}_j^\alpha\}](\mathbf{z}_a)]}{\text{Var}(\mathcal{I}_{\text{WF}}[\{\mathbf{U}_j^\alpha\}](\mathbf{z}_a))^{1/2}},$$

where \mathbf{z}_a is the true location of the inclusion. From (4.6), (4.7), and (5.13), we have

$$(5.14) \quad \text{SNR} = \frac{4\sqrt{2\pi^{d-2}n\omega^{5-d}\rho_0^3c_\alpha^{d-1}}\delta^d|B||\rho_1 - \rho_0|}{\sigma_{\text{noise}}} |\Im\{\mathbf{\Gamma}_{0,\alpha}^\omega(\mathbf{0})\}|.$$

From (5.14), the SNR is proportional to the contrast $|\rho_1 - \rho_0|$ and the volume of the inclusion $\delta^d|B|$ over the standard deviation of the noise, σ_{noise} .

5.3.2. Case II: Elasticity contrast. In the case of elastic contrast, the imaging functional becomes for $\mathbf{z} \in \Omega$

$$\mathcal{I}_{\text{WF}}[\{\mathbf{U}_j^\alpha\}](\mathbf{z}) = c_\alpha \frac{1}{n} \sum_{j=1}^n \nabla \mathbf{U}_j^\alpha(\mathbf{z}) : \mathbb{M}'(B')(\nabla \mathbf{w}_{j,\text{true}}^\alpha(\mathbf{z}) + \nabla \mathbf{w}_{j,\text{noise}}^\alpha(\mathbf{z})).$$

Here, $\mathbf{w}_{j,\text{true}}^\alpha$ and $\mathbf{w}_{j,\text{noise}}^\alpha$ are defined in the last section. They correspond to the backpropagation of pure data and that of the measurement noise. The contribution of $\mathbf{w}_{j,\text{true}}^\alpha$ is exactly the imaging functional with unperturbed data, and it is investigated in Proposition 4.2. The contribution of $\mathbf{w}_{j,\text{noise}}^\alpha$ perturbs the true image. For $\mathbf{z}, \mathbf{z}' \in \Omega$, the covariance function of the

TD noisy image is given by

$$\begin{aligned}
& \text{Cov}(\mathcal{I}_{\text{WF}}[\{\mathbf{U}_j^\alpha\}](\mathbf{z}), \mathcal{I}_{\text{WF}}[\{\mathbf{U}_j^\alpha\}](\mathbf{z}')) \\
&= c_\alpha^2 \frac{1}{n^2} \sum_{j,l=1}^n \mathbb{E}[\Re\{ \nabla \mathbf{U}_j^\alpha(\mathbf{z}) : \mathbb{M}' \nabla \mathbf{w}_{j,\text{noise}}^\alpha(\mathbf{z}) \} \Re\{ \nabla \mathbf{U}_l^\alpha(\mathbf{z}') : \mathbb{M}' \nabla \mathbf{w}_{l,\text{noise}}^\alpha(\mathbf{z}') \}] \\
&= c_\alpha^2 \frac{1}{2n^2} \sum_{j,l=1}^n \Re \mathbb{E}[(\nabla \mathbf{U}_j^\alpha(\mathbf{z}) : \mathbb{M}' \nabla \mathbf{w}_{j,\text{noise}}^\alpha(\mathbf{z})) \overline{(\nabla \mathbf{U}_l^\alpha(\mathbf{z}') : \mathbb{M}' \nabla \mathbf{w}_{l,\text{noise}}^\alpha(\mathbf{z}'))}] \\
&= c_\alpha^2 \frac{1}{2n^2} \sum_{j=1}^n \Re \left\{ \nabla \mathbf{U}_j^\alpha(\mathbf{z}) : \mathbb{M}' \left[\mathbb{E}[\nabla \mathbf{w}_{j,\text{noise}}^\alpha(\mathbf{z}) \overline{\nabla \mathbf{w}_{j,\text{noise}}^\alpha(\mathbf{z}')}] : \mathbb{M}' \overline{\nabla \mathbf{U}_j^\alpha(\mathbf{z}')} \right] \right\}.
\end{aligned}$$

Using (5.11), we find that

$$\mathbb{E}[\nabla \mathbf{w}_{j,\text{noise}}^\alpha(\mathbf{z}) \overline{\nabla \mathbf{w}_{j,\text{noise}}^\alpha(\mathbf{z}')}] = -\frac{\sigma_{\text{noise}}^2}{4c_\alpha \omega} \Im m \nabla_{\mathbf{z}} \nabla_{\mathbf{z}'} \{ \mathbf{\Gamma}_{0,\alpha}^\omega(\mathbf{z} - \mathbf{z}') \}.$$

After substituting this term into the expression of the covariance function, we find that it becomes

$$\frac{c_\alpha \sigma_{\text{noise}}^2}{4\omega} \frac{1}{2n} \sum_{j=1}^n \Re \left\{ \nabla \mathbf{U}_j^\alpha(\mathbf{z}) : \mathbb{M}' \left[\Im m \{ \nabla^2 \mathbf{\Gamma}_{0,\alpha}^\omega(\mathbf{z} - \mathbf{z}') \} : \mathbb{M}' \overline{\nabla \mathbf{U}_j^\alpha(\mathbf{z}')} \right] \right\}.$$

The sum has exactly the form that was analyzed in the proof of Proposition 3.4. Using similar techniques, we finally obtain that

$$(5.15) \quad \text{Cov}(\mathcal{I}_{\text{WF}}[\{\mathbf{U}_j^\alpha\}](\mathbf{z}), \mathcal{I}_{\text{WF}}[\{\mathbf{U}_j^\alpha\}](\mathbf{z}')) = \mu_0 \left(\frac{c_\alpha}{\omega} \right)^3 \left(\frac{\pi}{\kappa_\alpha} \right)^{d-2} \left(\frac{\kappa_S}{\kappa_\alpha} \right)^2 \frac{\sigma_{\text{noise}}^2}{2n} J_{\alpha,\alpha}(\mathbf{z}, \mathbf{z}'),$$

where $J_{\alpha,\alpha}$ is defined by (3.24). The variance of the TD image can also be obtained from (5.15). As in the case of density contrast, the typical shape of hot spots in the image corrupted by noise is the same as the main peak of the true image. Further, the effect of measurement noise is reduced by a factor of \sqrt{n} by using n plane waves. In particular, the SNR of the TD image is given by

$$(5.16) \quad \text{SNR} = \frac{\delta^d \sqrt{\mu_0 \omega}}{\sqrt{c_\alpha^3}} \left(\frac{\pi}{\kappa_\alpha} \right)^{\frac{d-2}{2}} \frac{\kappa_S}{\kappa_\alpha} \frac{4\sqrt{2n}}{\sigma_{\text{noise}}} \sqrt{J_{\alpha,\alpha}(\mathbf{z}_a, \mathbf{z}_a)}.$$

6. Statistical stability with medium noise. In the previous section, we demonstrated that the proposed imaging functional using multidirectional plane waves is statistically stable with respect to uncorrelated measurement noises. Now we investigate the case of medium noise, where the constitutive parameters of the elastic medium fluctuate around a constant background.

6.1. Medium noise model. For simplicity, we consider a medium that fluctuates in the density parameter only. That is,

$$(6.1) \quad \rho(\mathbf{x}) = \rho_0[1 + \gamma(\mathbf{x})],$$

where ρ_0 is the constant background and $\rho_0\gamma(\mathbf{x})$ is the random fluctuation in the density. Note that γ is real-valued.

Throughout this section, we will call the homogeneous medium with parameters $(\lambda_0, \mu_0, \rho_0)$ the reference medium. The background medium refers to the one without inclusion but with density fluctuation. Consequently, the background Neumann problem of elastic waves is no longer (2.21). Indeed, that equation corresponds to the reference medium, and its solution will be denoted by $\mathbf{U}^{(0)}$. The new background solution is

$$(6.2) \quad \begin{cases} (\mathcal{L}_{\lambda_0, \mu_0} + \rho_0\omega^2[1 + \gamma])\mathbf{U} = 0 & \text{on } \Omega, \\ \frac{\partial \mathbf{U}}{\partial \nu} = \mathbf{g} & \text{on } \partial\Omega. \end{cases}$$

Similarly, the Neumann function associated with the problem in the reference medium will be denoted by $\mathbf{N}^{\omega, (0)}$. We denote by \mathbf{N}^ω the Neumann function associated with the background medium, that is,

$$(6.3) \quad \begin{cases} (\mathcal{L}_{\lambda_0, \mu_0} + \rho_0\omega^2[1 + \gamma(\mathbf{x})])\mathbf{N}^\omega(\mathbf{x}, \mathbf{y}) = -\delta_{\mathbf{y}}(\mathbf{x})\mathbf{I}_2, & \mathbf{x} \in \Omega, \quad \mathbf{x} \neq \mathbf{y}, \\ \frac{\partial \mathbf{N}^\omega}{\partial \nu}(\mathbf{x}, \mathbf{y}) = 0, & \mathbf{x} \in \partial\Omega. \end{cases}$$

We assume that γ has small amplitude so that the Born approximation is valid. In particular, we have

$$(6.4) \quad \mathbf{N}^\omega(\mathbf{x}, \mathbf{y}) \simeq \mathbf{N}^{\omega, (0)}(\mathbf{x}, \mathbf{y}) + \rho_0\omega^2 \int_{\Omega} \mathbf{N}^{\omega, (0)}(\mathbf{x}, \mathbf{z})\gamma(\mathbf{z})\mathbf{N}^{\omega, (0)}(\mathbf{z}, \mathbf{y})d\mathbf{y}.$$

As a consequence, we also have that $\mathbf{U} \simeq \mathbf{U}^{(0)} - \mathbf{U}^{(1)}$, where

$$(6.5) \quad \mathbf{U}^{(1)}(\mathbf{x}) = -\rho_0\omega^2 \int_{\Omega} \mathbf{N}^{\omega, (0)}(\mathbf{x}, \mathbf{z})\gamma(\mathbf{z})\mathbf{U}^{(0)}(\mathbf{z})d\mathbf{z}.$$

Letting σ_γ denote the typical size of γ , the remainders in the above approximations are of order $o(\sigma_\gamma)$.

6.2. Statistics of the speckle field in the case of a density contrast only. We assume that the inclusion has density contrast only. The backpropagation step constructs \mathbf{w} as follows:

$$(6.6) \quad \mathbf{w}(\mathbf{x}) = \int_{\partial\Omega} \Gamma_0^\omega(\mathbf{x}, \mathbf{z}) \overline{\left(\frac{1}{2}I - \mathcal{K}_\Omega^{\omega, (0)}\right)} [\mathbf{U}^{(0)} - \mathbf{u}_{\text{meas}}](\mathbf{z})d\sigma(\mathbf{z}), \quad \mathbf{x} \in \Omega.$$

We emphasize that the backpropagation step uses the reference fundamental solutions, and the differential measurement is with respect to the reference solution. These are necessary

steps because of the fluctuation in the background medium or, equivalently, because of the fact that the background solution is unknown.

We write the difference between $\mathbf{U}^{(0)}$ and \mathbf{u}_{meas} as the sum of $\mathbf{U}^{(0)} - \mathbf{U}$ and $\mathbf{U} - \mathbf{u}_{\text{meas}}$. These two differences are estimated by $\mathbf{U}^{(1)}$ in (6.5) and by (2.22), respectively. Using Lemma 2.1, we find that

$$(6.7) \quad \begin{aligned} \mathbf{w}(\mathbf{x}) = & -\rho_0\omega^2 \int_{\partial\Omega} \Gamma_0^\omega(\mathbf{x} - \mathbf{z}) \int_{\Omega} \overline{\Gamma_0^\omega(\mathbf{z} - \mathbf{y})} \overline{\mathbf{U}^{(0)}(\mathbf{y})} \gamma(\mathbf{y}) d\mathbf{y} d\sigma(\mathbf{z}) \\ & - C\delta^d \int_{\partial\Omega} \Gamma_0^\omega(\mathbf{x} - \mathbf{z}) \overline{\Gamma_0^\omega(\mathbf{z} - \mathbf{z}_a)} \overline{\mathbf{U}^{(0)}(\mathbf{z}_a)} d\sigma(\mathbf{z}) + O(\sigma_\gamma\delta^d) + o(\sigma_\gamma), \quad \mathbf{x} \in \Omega, \end{aligned}$$

where $C = \omega^2(\rho_0 - \rho_1)|B|$. The second term is the leading contribution of $\mathbf{U} - \mathbf{u}_{\text{meas}}$ given by approximating the unknown Neumann function and the background solution by those associated with the reference medium. The leading error in this approximation is of order $O(\sigma_\gamma\delta^d)$ and can be written explicitly as

$$\begin{aligned} C\rho_0\omega^2\delta^d \int_{\partial\Omega} \Gamma_0^\omega(\mathbf{x}, \mathbf{z}) \int_{\Omega} \overline{\Gamma_0^\omega(\mathbf{z}, \mathbf{y})} \overline{\mathbf{N}^{\omega,(0)}(\mathbf{y}, \mathbf{z}_a)} \overline{\mathbf{U}^{(0)}(\mathbf{z}_a)} \gamma(\mathbf{y}) d\mathbf{y} d\sigma(\mathbf{z}) \\ - C\rho_0\omega^2\delta^d \int_{\partial\Omega} \Gamma_0^\omega(\mathbf{x}, \mathbf{z}) \overline{\Gamma_0^\omega(\mathbf{z}, \mathbf{z}_a)} \int_{\Omega} \overline{\mathbf{N}^{\omega,(0)}(\mathbf{z}_a, \mathbf{y})} \overline{\mathbf{U}^{(0)}(\mathbf{y})} \gamma(\mathbf{y}) d\mathbf{y} d\sigma(\mathbf{z}); \end{aligned}$$

it is neglected in what follows.

For the Helmholtz decomposition \mathbf{w}^α , $\alpha \in \{P, S\}$, the first fundamental solution $\Gamma_0^\omega(\mathbf{x} - \mathbf{z})$ in the expression (6.7) should be changed to $\Gamma_{0,\alpha}^\omega(\mathbf{x} - \mathbf{z})$. We observe that the second term in (6.7) is exactly (3.10). Therefore, we call this term \mathbf{w}_{true} and refer to the other term in the expression as $\mathbf{w}_{\text{noise}}$. Using the Helmholtz–Kirchhoff identity, we obtain

$$(6.8) \quad \mathbf{w}_{\text{noise}}^\alpha(\mathbf{x}) \simeq -\frac{\rho_0\omega}{c_\alpha} \int_{\Omega} \gamma(\mathbf{y}) \Im\{\Gamma_{0,\alpha}^\omega(\mathbf{x} - \mathbf{y})\} \overline{\mathbf{U}^{(0)}(\mathbf{y})} d\mathbf{y}, \quad \mathbf{x} \in \Omega.$$

We have decomposed the backpropagation \mathbf{w}^α into the “true” $\mathbf{w}_{\text{true}}^\alpha$, which behaves as in the reference medium, and the error part $\mathbf{w}_{\text{noise}}^\alpha$. In the TD imaging functional using multiple plane waves with equidistributed directions, the contribution of $\mathbf{w}_{\text{true}}^\alpha$ is exactly as the one analyzed in Proposition 4.1. The contribution of $\mathbf{w}_{\text{noise}}^\alpha$ is a speckle field.

The covariance function of this speckle field or, equivalently, that of the TD image corrupted by noise, is

$$\begin{aligned} \text{Cov}(\mathcal{I}_{\text{WF}}[\{\mathbf{U}_j^\alpha\}](\mathbf{z}), \mathcal{I}_{\text{WF}}[\{\mathbf{U}_j^\alpha\}](\mathbf{z}')) \\ = C_\alpha^2 \frac{1}{n^2} \sum_{j,l=1}^n \mathbb{E} \left[\Re \left\{ \mathbf{U}_j^{(0),\alpha}(\mathbf{z}) \cdot \mathbf{w}_{j,\text{noise}}^\alpha(\mathbf{z}) \right\} \Re \left\{ \mathbf{U}_l^{(0),\alpha}(\mathbf{z}') \cdot \mathbf{w}_{l,\text{noise}}^\alpha(\mathbf{z}') \right\} \right] \end{aligned}$$

for $\mathbf{z}, \mathbf{z}' \in \Omega$, where C_α is defined to be $c_\alpha\omega^2|B'|(\rho_1/\rho_0 - 1)$. Here $\mathbf{U}^{(0),\alpha}$ are the reference incoming plane waves (3.14).

Using the expression (6.8), we have

$$\begin{aligned} \frac{1}{n} \sum_{j=1}^n \mathbf{U}_j^\alpha(\mathbf{z}) \cdot \mathbf{w}_{j,\text{noise}}^\alpha(\mathbf{z}) &= -b_\alpha \frac{1}{n} \sum_{j=1}^n \int_{\Omega} \gamma(\mathbf{y}) \left[\mathbf{U}_j^{(0),\alpha}(\mathbf{z}) \otimes \overline{\mathbf{U}_j^{(0),\alpha}(\mathbf{y})} \right] : \Im m \{ \mathbf{\Gamma}_{0,\alpha}^\omega(\mathbf{z} - \mathbf{y}) \} d\mathbf{y} \\ &= -b_\alpha \int_{\Omega} \gamma(\mathbf{y}) \frac{1}{n} \sum_{j=1}^n e^{i\kappa_\alpha(\mathbf{z}-\mathbf{y}) \cdot \mathbf{e}_{\theta_j}} \mathbf{e}_{\theta_j}^\alpha \otimes \mathbf{e}_{\theta_j}^\alpha : \Im m \{ \mathbf{\Gamma}_{0,\alpha}^\omega(\mathbf{z} - \mathbf{y}) \} d\mathbf{y}, \end{aligned}$$

where $b_\alpha = (\rho_0\omega)/c_\alpha$. Finally, using (3.18) and (3.19) for $\alpha = P$ and S , respectively, we obtain that

$$(6.9) \quad \frac{1}{n} \sum_{j=1}^n \mathbf{U}_j^{(0),\alpha}(\mathbf{z}) \cdot \mathbf{w}_{j,\text{noise}}^\alpha(\mathbf{z}) = b'_\alpha \int_{\Omega} \gamma(\mathbf{y}) |\Im m \{ \mathbf{\Gamma}_{0,\alpha}^\omega(\mathbf{z} - \mathbf{y}) \}|^2 d\mathbf{y}.$$

Here $b'_\alpha = 4b_\alpha\mu_0\left(\frac{\pi}{\kappa_\alpha}\right)^{d-2}\left(\frac{\kappa_S}{\kappa_\alpha}\right)^2$. Note that the sum above is a real quantity.

The covariance function of the TD image simplifies to

$$(6.10) \quad C_\alpha^2 b_\alpha'^2 \int_{\Omega} \int_{\Omega} C_\gamma(\mathbf{y}, \mathbf{y}') |\Im m \{ \mathbf{\Gamma}_{0,\alpha}^\omega(\mathbf{z} - \mathbf{y}) \}|^2 |\Im m \{ \mathbf{\Gamma}_{0,\alpha}^\omega(\mathbf{z}' - \mathbf{y}') \}|^2 d\mathbf{y} d\mathbf{y}',$$

where $C_\gamma(\mathbf{y}, \mathbf{y}') = \mathbb{E}[\gamma(\mathbf{y})\gamma(\mathbf{y}')] is the two-point correlation function of the fluctuations in the density parameter.$

Remark 6.1. The expression in (6.9) shows that the speckle field in the image is essentially the medium noise smoothed by an integral kernel of the form $|\Im m \mathbf{\Gamma}_{0,\alpha}^\omega|^2$. Similarly, (6.10) shows that the correlation structure of the speckle field is essentially that of the medium noise smoothed by the same kernel. Because the typical width of this kernel is about half the wavelength, the correlation length of the speckle field is roughly the maximum between the correlation length of medium noise and the wavelength.

6.3. Statistics of the speckle field in the case of an elasticity contrast. The case of elasticity contrast can be considered similarly. The covariance function of the TD image is

$$c_\alpha^2 \frac{1}{n^2} \sum_{j,l=1}^n \mathbb{E} \left[\Re e \left\{ \nabla \mathbf{U}_j^{(0),\alpha}(\mathbf{z}) : \mathbb{M}' \nabla \mathbf{w}_{j,\text{noise}}^\alpha(\mathbf{z}) \right\} \Re e \left\{ \nabla \mathbf{U}_l^{(0),\alpha}(\mathbf{z}') : \mathbb{M}' \nabla \mathbf{w}_{l,\text{noise}}^\alpha(\mathbf{z}') \right\} \right].$$

Using the expression of $\mathbf{w}_{\text{noise}}^\alpha$, we have

$$\begin{aligned} \frac{1}{n} \sum_{j=1}^n \nabla \mathbf{U}_j^\alpha(\mathbf{z}) : \mathbb{M}' \nabla \mathbf{w}_{j,\text{noise}}^\alpha(\mathbf{z}) &= -b_\alpha \int_{\Omega} \gamma(\mathbf{y}) \frac{1}{n} \sum_{j=1}^n i\kappa_\alpha e^{i\kappa_\alpha(\mathbf{z}-\mathbf{y}) \cdot \mathbf{e}_{\theta_j}} \\ &\quad \times \mathbf{e}_{\theta_j} \otimes \mathbf{e}_{\theta_j}^\alpha \otimes \mathbf{e}_{\theta_j}^\alpha : [\mathbb{M}' \Im m \{ \nabla_{\mathbf{z}} \mathbf{\Gamma}_{0,\alpha}^\omega(\mathbf{z} - \mathbf{y}) \}] d\mathbf{y}. \end{aligned}$$

From (3.18) and (3.19), we see that

$$(6.11) \quad \frac{1}{n} \sum_{j=1}^n i\kappa_\alpha e^{i\kappa_\alpha \mathbf{x} \cdot \mathbf{e}_{\theta_j}} \mathbf{e}_{\theta_j} \otimes \mathbf{e}_{\theta_j}^\alpha \otimes \mathbf{e}_{\theta_j}^\alpha = -4\mu_0 \left(\frac{\pi}{\kappa_\alpha} \right)^{d-2} \left(\frac{\kappa_S}{\kappa_\alpha} \right)^2 \Im m \{ \nabla \mathbf{\Gamma}_{0,\alpha}^\omega(\mathbf{x}) \}.$$

Using this formula, we get

$$(6.12) \quad \frac{1}{n} \sum_{j=1}^n \nabla \mathbf{U}_j^\alpha(\mathbf{z}) : \mathbb{M}' \nabla \mathbf{w}_{j,\text{noise}}^\alpha(\mathbf{z}) = b'_\alpha \int_{\Omega} \gamma(\mathbf{y}) Q_\alpha^2[\mathbb{M}'](\mathbf{z} - \mathbf{y}) d\mathbf{y},$$

where $Q_\alpha^2[\mathbb{M}'](\mathbf{x})$ is a nonnegative function defined as

$$(6.13) \quad \begin{aligned} Q_P^2[\mathbb{M}](\mathbf{x}) &= \Im\{\nabla \mathbf{\Gamma}_{0,P}^\omega(\mathbf{x})\} : [\mathbb{M} \Im\{\nabla \mathbf{\Gamma}_{0,P}^\omega(\mathbf{x})\}] \\ &= a |\Im\{\nabla \mathbf{\Gamma}_{0,P}^\omega(\mathbf{x})\}|^2 + b |\Im\{\nabla \cdot \mathbf{\Gamma}_{0,P}^\omega(\mathbf{x})\}|^2. \end{aligned}$$

The last equality follows from the expression (2.19) of \mathbb{M} and the fact that $\partial_i(\mathbf{\Gamma}_{0,P}^\omega)_{jk} = \partial_j(\mathbf{\Gamma}_{0,P}^\omega)_{ik}$. This symmetry is not satisfied for $\mathbf{\Gamma}_{0,P}^\omega$, for which we have

$$(6.14) \quad \begin{aligned} Q_S^2[\mathbb{M}](\mathbf{x}) &= \Im\{\nabla \mathbf{\Gamma}_{0,S}^\omega(\mathbf{x})\} : [\mathbb{M} \Im\{\nabla \mathbf{\Gamma}_{0,S}^\omega(\mathbf{x})\}] \\ &= \frac{a}{2} |\Im\{\nabla \mathbf{\Gamma}_{0,S}^\omega(\mathbf{x})\}|^2 + \frac{a}{2} \Im\{\nabla \mathbf{\Gamma}_{0,S}^\omega(\mathbf{x})\} : \Im\{\tilde{\nabla} \mathbf{\Gamma}_{0,S}^\omega(\mathbf{x})\} + b |\Im\{\nabla \cdot \mathbf{\Gamma}_{0,S}^\omega(\mathbf{x})\}|^2. \end{aligned}$$

Here $(\nabla \cdot \mathbf{\Gamma}_{0,S}^\omega)_{jkl} = \partial_k(\mathbf{\Gamma}_{0,S}^\omega)_{jl}$. Note that Q_α^2 is nonnegative and (6.12) is real-valued. The covariance function of the TD image simplifies to

$$(6.15) \quad c_\alpha^2 b_\alpha'^2 \int_{\Omega} \int_{\Omega} C_\gamma(\mathbf{y}, \mathbf{y}') Q_\alpha^2[\mathbb{M}'](\mathbf{z} - \mathbf{y}) Q_\alpha^2[\mathbb{M}](\mathbf{z}' - \mathbf{y}') d\mathbf{y} d\mathbf{y}', \quad \mathbf{z}, \mathbf{z}' \in \Omega.$$

Remark 6.2. If we compare (6.12) with (6.9), then one can see that they are of the same form except that the integral kernel is now $Q_\alpha^2[\mathbb{M}']$. Therefore, Remark 6.1 applies here as well. We remark also that the further reduction of the effect of measurement noise with rate $1/\sqrt{2n}$ does not appear in the medium noise case. In this sense, TD imaging is less stable with respect to medium noise.

6.4. Random elastic medium. In this section we consider the case when the random fluctuation occurs in the elastic coefficients. This is a more delicate case because it is well known that inhomogeneity in the Lamé coefficients cause mode conversion. Nevertheless, we demonstrate below that as long as the random fluctuation is weak so that the Born approximation is valid, the imaging functional we proposed remains stable.

To simplify the presentation, we assume that random fluctuation occurs only in the shear modulus μ while the density ρ_0 and the first Lamé coefficient λ_0 are homogeneous. The equation for a time-harmonic elastic wave is then

$$(6.16) \quad \rho_0 \omega^2 \mathbf{u} + \lambda_0 \nabla(\nabla \cdot \mathbf{u}) + \nabla \cdot [\mu(\mathbf{x})(\nabla \mathbf{u} + (\nabla \mathbf{u})^T)] = 0,$$

with the same boundary condition as before. The inhomogeneous shear modulus is given by

$$(6.17) \quad \mu(\mathbf{x}) = \mu_0 + \gamma(\mathbf{x}, \omega),$$

where $\gamma(\mathbf{x})$ is a random process modeling the fluctuation.

Born approximation. The equation for the elastic wave above can be written as

$$\mathcal{L}_{\lambda_0, \mu_0} \mathbf{u} + \rho_0 \omega^2 \mathbf{u} = -\nabla \cdot [\gamma(\mathbf{x})(\nabla \mathbf{u} + (\nabla \mathbf{u})^T)].$$

Assume that the random fluctuation γ is small enough so that the Born approximation is valid. We then have $\mathbf{u} \simeq \mathbf{u}_0 - \mathbf{u}_1$, where \mathbf{u}_0 solves the equation in the background medium and \mathbf{u}_1 , the first scattering, solves the above equation with \mathbf{u} on the right-hand side replaced by \mathbf{u}_0 . More precisely, we have

$$(6.18) \quad \mathbf{u}_1(\mathbf{x}) = \int_{\Omega} \mathbf{N}^\omega(\mathbf{x}, \mathbf{y}) \nabla \cdot [\gamma(\mathbf{y})(\nabla \mathbf{u}_0 + (\nabla \mathbf{u}_0)^T)] d\mathbf{y}.$$

Here, \mathbf{N}^ω is the Neumann function in the background medium without random fluctuation.

Postprocessing step. As seen before, the postprocessing (3.6) is a critical step in our method. As discussed in section 6.2, even when the medium is random, we have to use the reference Green function and the reference solution associated with the homogeneous medium in this postprocessing step. Following the analysis in section 6.2, we see that as in (6.7) the function \mathbf{w} contains two main contributions: First, backpropagating the difference between the measurement and the background solution in the random medium but without inclusion contributes to the detection of inclusion. Second, backpropagating the difference between the background solution and the reference solution in the homogeneous medium amounts to a speckle pattern in the image.

The first contribution corresponds to the case with exact data and is discussed in section 4. We focus on the second contribution, which accounts for the statistical stability. This part of the postprocessed function \mathbf{w} has the expression

$$\begin{aligned} \mathbf{w}_{\text{noise}}^\alpha(\mathbf{z}) &= \mathcal{H}^\alpha \left[\mathcal{S}_\Omega^\omega \left(\frac{1}{2} I - \mathcal{K}_\Omega^\omega \right) \mathbf{u}_1 \right] \\ &= \mathcal{H}^\alpha \left[\int_{\partial\Omega} \mathbf{\Gamma}_0^\omega(\mathbf{z}, \mathbf{y}) \left[\left(\frac{1}{2} I - \mathcal{K}_\Omega^\omega \right) \int_{\Omega} \mathbf{N}^\omega(\cdot, \mathbf{x}) \mathbf{v}(\mathbf{x}) d\mathbf{x} \right] (\mathbf{y}) d\sigma(\mathbf{y}) \right] \\ &= \int_{\partial\Omega} \mathbf{\Gamma}_{0,\alpha}^\omega(\mathbf{z}, \mathbf{y}) \int_{\Omega} \overline{\mathbf{\Gamma}_0^\omega(\mathbf{y}, \mathbf{x})} \nabla \cdot [\gamma(\mathbf{x}) \overline{(\nabla \mathbf{u}_0 + (\nabla \mathbf{u}_0)^T)}(\mathbf{x})] d\mathbf{x} d\sigma(\mathbf{y}). \end{aligned}$$

In the second equality above, $\mathbf{v}(\mathbf{x})$ is a short-hand notation for the divergence term in the line below. We refer to this term as the first scattering source. Using the Helmholtz–Kirchhoff identity again, we obtain that

$$(6.19) \quad \mathbf{w}_{\alpha, \text{noise}}(\mathbf{z}) = \frac{1}{c_\alpha \omega} \int_{\Omega} \Im m \{ \mathbf{\Gamma}_{0,\alpha}^\omega(\mathbf{z}, \mathbf{x}) \} \nabla \cdot [\gamma(\mathbf{x}) \overline{(\nabla \mathbf{u}_0 + (\nabla \mathbf{u}_0)^T)}(\mathbf{x})] d\mathbf{x}.$$

Remark 6.3. Compare the above expression with that in (6.8). The first scattering source in (6.8) is exactly the incident wave in the case with density fluctuation but is more complicated in the case with elastic fluctuation; see (6.20) below. This shows that the Born approximation in an inhomogeneous medium indeed captures weak mode conversion. Nevertheless, (6.19) shows that our method, due to the Helmholtz–Kirchhoff identity and our proposal of using

Helmholtz decomposition, extracts only the modes that are desired by the imaging functional. As we will see, this is crucial to the statistical stability of the imaging functional.

The speckle field. For simplicity of presentation, we consider only the case of density inclusion and the usage of pressure waves in (5.1). For a pressure wave $\mathbf{U}^P = e^{i\kappa_P \mathbf{x} \cdot \mathbf{e}_\theta}$, the first scattering source is

$$(6.20) \quad \mathbf{v}(\mathbf{x}) = 2i\kappa_P \nabla \cdot (\gamma(\mathbf{x}) e^{i\kappa_P \mathbf{x} \cdot \mathbf{e}_\theta} \mathbf{e}_\theta \otimes \mathbf{e}_\theta) = 2i\kappa_P (\nabla \gamma \cdot \mathbf{e}_\theta) \mathbf{U}^P(\mathbf{x}) - 2\kappa_P^2 \gamma(\mathbf{x}) \mathbf{U}^P(\mathbf{x}).$$

The speckle field in the imaging functional with a set of pressure waves $\{\mathbf{U}_j^P\}$ is

$$\begin{aligned} \mathcal{I}_{\text{WF,noise}}[\{\mathbf{U}_j^P\}](\mathbf{z}) &= c_P \omega^2 \left(\frac{\rho'_1}{\rho_0} - 1 \right) |B'| \frac{1}{n} \Re e \sum_{j=1}^n \mathbf{U}_j^P(\mathbf{z}) \cdot \mathbf{w}_{\text{noise}}^P(\mathbf{z}) \\ &= \omega \left(\frac{\rho'_1}{\rho_0} - 1 \right) |B'| \Re e \int_{\Omega} -2\kappa_P^2 \gamma(\mathbf{x}) \frac{1}{n} \sum_{j=1}^n e^{i\kappa_P(\mathbf{z}-\mathbf{x}) \cdot \mathbf{e}_{\theta_j}} \mathbf{e}_{\theta_j} \otimes \mathbf{e}_{\theta_j} : \Im m \{ \mathbf{\Gamma}_{0,P}^\omega(\mathbf{z}, \mathbf{x}) \} \\ &\quad - 2 \frac{1}{n} \sum_{j=1}^n i\kappa_P e^{i\kappa_P(\mathbf{z}-\mathbf{x}) \cdot \mathbf{e}_{\theta_j}} \mathbf{e}_{\theta_j} \otimes \mathbf{e}_{\theta_j} \otimes \mathbf{e}_{\theta_j} : [\nabla \gamma(\mathbf{x}) \otimes \Im m \{ \mathbf{\Gamma}_{0,P}^\omega(\mathbf{z}, \mathbf{x}) \}] d\mathbf{x}. \end{aligned}$$

Using the summation formulas (3.18) and (6.11), we can rewrite the above quantity as

$$C_1^P \int_{\Omega} 2\kappa_P^2 \gamma(\mathbf{x}) |\Im m \{ \mathbf{\Gamma}_{0,P}^\omega(\mathbf{z}, \mathbf{x}) \}|^2 + 2 \Im m \{ \nabla_{\mathbf{z}} \mathbf{\Gamma}_{0,P}^\omega(\mathbf{z}, \mathbf{x}) \} : [\nabla \gamma(\mathbf{x}) \otimes \Im m \{ \mathbf{\Gamma}_{0,P}^\omega(\mathbf{z}, \mathbf{x}) \}] d\mathbf{x}.$$

Here, the constant is

$$C_1^P = 4\mu_0 \left(\frac{\pi}{\kappa_P} \right)^{d-2} \left(\frac{\kappa_S}{\kappa_P} \right)^2 \omega \left(\frac{\rho'_1}{\rho_0} - 1 \right) |B'| = 4\pi^{d-2} \frac{\omega^3}{\kappa_P^d} (\rho'_1 - \rho_0) |B'|.$$

Assuming that $\gamma = 0$ near the boundary and using the divergence theorem, we can further simplify the expression of the speckle field to

$$C_1^P \int_{\Omega} \gamma(\mathbf{x}) [(2\kappa_P^2 I + \Delta_{\mathbf{x}}) |\Im m \{ \mathbf{\Gamma}_{0,P}^\omega(\mathbf{z}, \mathbf{x}) \}|^2] d\mathbf{x} = C_1^P \int_{\Omega} [(2\kappa_P^2 I + \Delta) \gamma(\mathbf{x})] |\Im m \{ \mathbf{\Gamma}_{0,P}^\omega(\mathbf{z}, \mathbf{x}) \}|^2 d\mathbf{x}.$$

This expression is again of the form of (6.9) and (6.12) except that the integral kernel is more complicated. Its correlation can be similarly calculated. Furthermore, Remarks 6.1 and 6.3 apply here.

Remark 6.4. For other settings such as elastic inclusion or when a set of shear waves are used in the imaging functional, the expressions for the speckle field and its statistics are more complicated. Explicit formulas for such settings are listed in [3], which is a longer version of this paper. Nevertheless, the salient feature of the speckle field does not change. It is essentially the medium noise (or the gradient of the medium noise) smoothed by an integral kernel whose width is of the order of the wavelength. The correlation length of the speckle field is of the order of the maximum between that of the medium noise and the wavelength.

7. Conclusion. In this paper, we performed an analysis of the topological derivative (TD) based elastic inclusion detection algorithm. We have seen that the standard TD based imaging functional may not attain its maximum at the location of the inclusion. Moreover, we have shown that its resolution does not reach the diffraction limit and identified the responsible terms, which are associated with the coupling of different wave modes. In order to enhance resolution to its optimum, we cancelled out these coupling terms by means of a Helmholtz decomposition, thereby designing a weighted imaging functional. We proved that the modified functional behaves like the square of the imaginary part of a pressure or a shear Green function, depending upon the choice of the incident wave, and then attains its maximum at the true location of the inclusion with a Rayleigh resolution limit, that is, of the order of half a wavelength. Finally, we have shown that the proposed imaging functionals are very stable with respect to measurement noise and moderately stable with respect to medium noise.

In a forthcoming work, we intend to extend the results of the paper to the localization of the small infinitesimal elastic cracks and to the case of elastostatics. In this regard recent contributions [11, 6, 10] are expected to play a key role.

REFERENCES

- [1] K. AKI AND P. G. RICHARDS, *Quantitative Seismology*, Vol. 1, W. H. Freeman & Co., San Francisco, 1980.
- [2] H. AMMARI, *An Introduction to Mathematics of Emerging Biomedical Imaging*, Math. Appl. (Berlin) 62, Springer-Verlag, Berlin, 2008.
- [3] H. AMMARI, E. BRETIN, J. GARNIER, W. JING, H. KANG, AND A. WAHAB, *Localization, Stability, and Resolution of Topological Derivative Based Imaging Functionals in Elasticity*, preprint, arXiv:1210.6760 [math.AP], 2012.
- [4] H. AMMARI, E. BRETIN, J. GARNIER, AND A. WAHAB, *Time reversal algorithms in viscoelastic media*, European J. Appl. Math., 24 (2013), pp. 565–600.
- [5] H. AMMARI, P. CALMON, AND E. IAKOVLEVA, *Direct elastic imaging of a small inclusion*, SIAM J. Imaging Sci., 1 (2008), pp. 169–187.
- [6] H. AMMARI, J. GARNIER, V. JUGNON, AND H. KANG, *Stability and resolution analysis for a topological derivative based imaging functional*, SIAM J. Control Optim., 50 (2012), pp. 48–76.
- [7] H. AMMARI, L. GUADARRAMA BUSTOS, H. KANG, AND H. LEE, *Transient elasticity imaging and time reversal*, Proc. Roy. Soc. Edinburgh Sect. A, 141 (2011), pp. 1121–1140.
- [8] H. AMMARI AND H. KANG, *Boundary layer techniques for solving the Helmholtz equation in the presence of small inhomogeneities*, J. Math. Anal. Appl., 296 (2004), pp. 190–208.
- [9] H. AMMARI AND H. KANG, *Reconstruction of Small Inhomogeneities from Boundary Measurements*, Lecture Notes in Math. 1846, Springer-Verlag, Berlin, 2004.
- [10] H. AMMARI AND H. KANG, *Polarization and Moment Tensors: With Applications to Inverse Problems and Effective Medium Theory*, Appl. Math. Sci. 162, Springer-Verlag, New York, 2007.
- [11] H. AMMARI, H. KANG, H. LEE, AND J. LIM, *Boundary perturbations due to the presence of small linear cracks in an elastic body*, J. Elasticity, 113 (2013), pp. 75–91.
- [12] H. AMMARI, H. KANG, G. NAKAMURA, AND K. TANUMA, *Complete asymptotic expansions of solutions of the system of elastostatics in the presence of inhomogeneities of small diameter*, J. Elasticity, 67 (2002), pp. 97–129.
- [13] J. CÉA, S. GARREAU, P. GUILLAUME, AND M. MASMOUDI, *The shape and topological optimization connection*, Comput. Methods Appl. Mech. Engrg., 188 (2001), pp. 703–726.
- [14] N. DOMINGUEZ AND V. GIBIAT, *Non-destructive imaging using the time domain topological energy method*, Ultrasonics, 50 (2010), pp. 367–372.
- [15] N. DOMINGUEZ, V. GIBIAT, AND Y. ESQUERREA, *Time domain topological gradient and time reversal analogy: An inverse method for ultrasonic target detection*, Wave Motion, 42 (2005), pp. 31–52.

- [16] A. ESCHENAUER, V. V. KOBELEV, AND A. SCHUMACHER, *Bubble method for topology and shape optimization of structures*, Struct. Optim., 8 (1994), pp. 42–51.
- [17] G. P. GALDI, *An Introduction to the Mathematical Theory of the Navier-Stokes Equations. Vol. I, Linearized Steady Problems*, Springer-Verlag, New York, 1994.
- [18] B. B. GUZINA AND M. BONNET, *Topological derivative for the inverse scattering of elastic waves*, Quart. J. Mech. Appl. Math., 57 (2004), pp. 161–179.
- [19] B. B. GUZINA AND I. CHIKICHEV, *From imaging to material identification: A generalized concept of topological sensitivity*, J. Mech. Phys. Solids, 55 (2007), pp. 245–279.
- [20] M. HINTERMÜLLER AND A. LAURAIN, *Electrical impedance tomography: From topology to shape*, Control Cybernet., 37 (2008), pp. 913–933.
- [21] M. HINTERMÜLLER, A. LAURAIN, AND A. A. NOVOTNY, *Second-order topological expansion for electrical impedance tomography*, Adv. Comput. Math., 36 (2012), pp. 235–265.
- [22] V. A. KORNEEV AND L. R. JOHNSON, *Scattering of P and S waves by a spherically symmetric inclusion*, Pure Appl. Geophys., 147 (1996), pp. 675–718.
- [23] V. D. KUPRADZE, *Potential Methods in the Theory of Elasticity*, Daniel Davey & Co., New York, 1965.
- [24] M. MASMOUDI, J. POMMIER, AND B. SAMET, *The topological asymptotic expansion for the Maxwell equations and some applications*, Inverse Problems, 21 (2005), pp. 547–564.
- [25] J. SOKOTOWSKI AND A. ŻOCHOWSKI, *On the topological derivative in shape optimization*, SIAM J. Control Optim., 37 (1999), pp. 1251–1272.
- [26] H. YUAN, B. B. GUZINA, AND R. SINKUS, *Application of topological sensitivity towards tissue elasticity imaging using magnetic resonance data*, J. Eng. Mech., to appear.